Macromolecular Materials and Engineering
Open Access
www.mame-journal.de

Electrospun Nanofiber Platforms for Photodynamic Therapy: Role and Efficacy in Cancer, Antimicrobial, and Wound Healing Applications

Aslı Eldem, Yamaç Tekintaş, Muhammed Ucuncu, and Nesrin Horzum**

Electrospinning offers a versatile platform for developing nanofibrous scaffolds capable of enhancing the therapeutic potential of photodynamic therapy (PDT). Photosensitizer (PS) loaded fibers exhibit a high surface area-to-volume ratio, promoting efficient drug delivery, prolonged retention at the target site, and controlled release profiles. Inducing reactive oxygen species (ROS) generation through light activation offers a targeted therapeutic approach, selectively generating cytotoxic effects in cancerous or pathogenic cells while minimizing damage to healthy tissue. This selective cytotoxicity arises because the ROS are produced only in illuminated areas where PS releases and accumulates, limiting their harmful effects to desired regions. Additionally, PS-loaded fibers are highly effective in wound healing applications, promoting cell proliferation and tissue regeneration while providing a barrier against microbial infections. This review highlights recent advances in the design and biomedical application of PS-loaded nanofibers, emphasizing their influence on cell viability and effectiveness in microbial inhibition, thereby setting the stage for future innovations in cancer therapy, wound healing, and infection control.

1. Introduction

1.1. A Historical Overview and Technological Progress in Electrospinning

1.1.1. History

Electrospinning uses an electric field to transform a polymer solution or melt into submicron and nano-sized fibers. It plays an important role in materials science and biomedical engineering and offers advantages such as large surface area, high porosity, and tunable physical properties.[1] The advancement of electrospinning techniques has reached critical milestones over the years. Lord Rayleigh reported the theoretical work studying the behavior of charged liquid jets.[2,3] In the early 1900s, John Cooley[4] and William J. Morton[5] patented some of the first methods of using electrical forces to draw thin fibers from liquids. In 1914, John Zeleny provided early insights into the mechanism of electrospinning.[6] Another significant advance in 1934 was when Anton Formhals patented the first electrospinning process, electrostatic forces were used to produce polymer filaments.[7] In 1966, Sir Geoffrey Ingram Taylor contributed his work on the "Taylor cone," which explained the jet formation process critical to electrospinning.[8] However, by the 1990s, interest in electrospinning waned, probably due to the difficulties in analyzing fiber morphology and measuring diameters at the submicron scale.[9]

The 1990s were driven by the rise of nanotechnology and were buoyed by innovations such as coaxial electrospinning for core-shell nanofibers. The term "electrospinning" was first used in the Web of Science in a conference paper by Jayesh Doshi and Darrell H. Reneker in 1993.[10] In 1999, Reneker started to utilize advancements in SEM to conduct a more detailed investigation into the parameters influencing the electrospinning process.[11] During the 2000s, this technique was further developed and electroblowing was introduced to better control fiber morphology and production speed.[12,13] In addition, Elmarco Corporation developed the Nanospider^{TM} for the first industrial-scale production of nanofibers. Furthermore, multi-needle [14] and needleless[15] electrospinning systems were reported, making large-scale production more feasible. Moreover, precise patterning of nanofibers was enabled by near-field electrospinning.[16]

A. Eldem, M. Ucuncu
Department of Analytical Chemistry, Faculty of Pharmacy
İzmir Katip,Çelebi University
İzmir 35620, Türkiye
E-mail: muhammed.ucuncu@ikcu.edu.tr
Y. Tekintaş
Department of Pharmaceutical Microbiology, Faculty of Pharmacy
İzmir Katip Çelebi University
İzmir 35620, Türkiye
N. Horzum
Department of Engineering Sciences, Faculty of Engineering and Architecture
İzmir Katip Çelebi University
İzmir 35620, Türkiye
E-mail: nesrin.horzum.polat@ikcu.edu.tr

The ORCID identification number(s) for the author(s) of this article can be found under https://doi.org/10.1002/mame.202500014

DOI: 10.1002/mame.202500014

In the 2020s, recent advances in the fabrication of 3D structures and smart materials have expanded the use of electrospun fibers in energy storage, environmental remediation, and advanced textiles, making the technology more commercially viable and versatile.[17]

1.1.2. Fundamentals of Electrospinning

The process of electrospinning involves a basic setup with four key elements: a high-voltage power supply, a syringe pump, a nozzle (syringe needle or metallic capillary), and a fiber collector (aluminum foil, rotating drum, flat plate, or wire mesh). A polymer dissolved in a solvent or solvent mixture is ejected from the syringe at a controlled rate adjusted by the syringe pump. The electrostatic force causes charge separation within the liquid, leading to the formation of a charged droplet at the tip of the nozzle. As the intensity of the electrostatic field increases, the surface charge density on the droplet enhances, causing the droplet to expand and transform into a Taylor cone. Eventually, electrostatic repulsion surpasses surface tension, and a jet forms, rapidly moving toward the collector. During this process, the polymer solution stretches and undergoes whipping, while the solvent evaporates, forming ultrafine fibers.[18,19]

The electrospinning process consists of four main stages: Taylor cone formation, jet ejection, jet stretching, and fiber solidification. A well-formed Taylor cone is crucial for producing uniform nanofibers, while irregular cones can lead to defects. The jet initially moves in a straight line, and its length affects fiber diameter. As the jet accelerates, the diameter decreases leading to fiber variations due to instability caused by electrostatic repulsion. There are three types of instabilities: Rayleigh, axisymmetric, and non-axisymmetric whipping. Rayleigh instability leads to the formation of beads on fibers, while subsequent axisymmetric instability causes the jet to form loops or coils due to electrostatic repulsion, resulting in jet thinning while retaining an axisymmetric pattern. However, non-axisymmetric whipping instability is key for reducing fiber diameter to the nanoscale. The solidification occurs through solvent evaporation, and slower rates yield thinner fibers.[20,21]

The optimization of electrospinning conditions is central to the efforts of researchers to produce nanofibers with specific morphologies and desired properties for bespoke applications. The critical variables can be categorized into three main groups. The first group, known as solution parameters, includes viscosity, molecular weight, concentration, conductivity, surface tension, and solvent type. The second group comprises process parameters, including the flow rate, applied voltage, the distance between the needle and collector, the design of the needle, and the collector type. The last group includes ambient parameters, such as temperature, relative humidity, and atmosphere type, which also significantly affect the process.[22]

The interconnected parameters of viscosity, molecular weight, and concentration of the solution play a vital role in determining the electrospinnability and final morphology of nanofibers. Among these, concentration is one of the significant parameters for optimizing the fiber structure, as it affects the viscosity, elasticity, and surface tension of the solution. If the solution is too dilute, the polymer chains do not overlap, resulting in viscoelasticity influenced by shorter polymer chains, and the droplet forms (electrospraying) instead of producing continuous fibers. A slight increase in concentration may fabricate beaded fibers, while a critical concentration promotes chain entanglement, resulting in bead-free nanofibers. However, excessively high concentrations can lead to increased viscosity, making them unsuitable for electrospinning and resulting in larger fiber diameters.[23,24]

To produce finer fibers during electrospinning, extending fiber elongation or flight time can be achieved by increasing the distance between the needle and the collector. This also helps to boost solvent evaporation, especially with low-volatility solvents and higher chamber temperatures. However, exceeding a critical working distance can destabilize the Taylor cone, causing uneven fibers.[25] Additionally, insufficient solvent volatility and low temperatures may lead to fiber fusion during deposition. Another process parameter is the electric field, which initiates jet formation in the polymer solution. A critical voltage, influenced by the surface tension of the solution, needs to be surpassed for jet generation. Increasing the voltage beyond this threshold typically reduces the flight time, leading to unstable paths and thicker fibers or secondary morphologies. Conversely, if the voltage is too low, the solution may spray onto the collector.[9] Besides applied voltage, the solution flow rate is a critical parameter that significantly impacts nanofiber morphology and diameter. Lower flow rates typically result in smaller and more uniform fibers as they allow adequate time for solvent evaporation. However, if the flow rate is too low, the jet becomes unstable, leading to beaded fibers or needle blockage. In contrast, increasing the flow rate produces thicker fibers, but excessively high rates can cause beaded fibers due to Taylor cone instability and insufficient evaporation time. The geometry of the collector and the design of the needle are also crucial for enhancing the orientation and properties of electrospun nanofibers. Modifications to collector geometry, such as rotating (drum, disc, rod) and conical mandrel, leverage high speeds and mechanical forces to align fibers, with a fast-moving substrate controlling the deposition pattern of the jet. The rotational speed significantly influences fiber diameter and alignment; higher speeds can yield smaller diameters, but exceeding a critical threshold risks fiber breakup.[25,26] Furthermore, parallel collectors offer an easy alternative to achieve highly aligned electrospun fibers using two electrodes separated by a void gap.[27,28] Unlike rotating collectors that depend on mechanical force, parallel collectors align fibers through electric fields, providing controlled orientation. Besides rotating and parallel collectors or magneto-electrospinning, adding magnetic fluid/nanoparticles to the spinning solution enables alignment when subjected to an external magnetic field, and focuses on fiber composition to respond directly to the field.[29] In addition to these conventional techniques, near-field electrospinning and 3D printing electrospinning techniques have been developed to achieve the ordered alignment of nanofibers.[30]

During electrospinning, temperature and humidity significantly influence fiber formation. Temperature impacts viscosity, surface tension, and evaporation rate, affecting jet solidification. High humidity can reduce charge density, causing nonuniformity, where low humidity shortens the jet path, resulting in thicker fibers. Additionally, in hygroscopic polymers, high humidity leads to unique fiber structures like porous or dimpled fibers.[31,32]

Table 1. Classification of electrospun nanofibers based on material composition, structure, functionalization, and alignment.

	Types of electrospun nanofibers		
Composition	Polymeric (natural, synthetic biodegradable)		
	Carbon		
	Composite (metal/metal oxide, carbon-based nanomaterials, drugs, bioceramics, dyes, antimicrobial and antioxidant agents)		
	Ceramic		
	Metallic		
Structure	Monolithic	Hollow/Tube	Island-like
	Co-axial (Core-shell)	Janus	Beads-in-fiber
	Multi-axial	Porous	Necklace-like
	Multichannel	Helical	Shish-kebap
Functionalization	Surface-modified (e.g., chemical groups, nanoparticles, active molecules)		
	Stimuli-responsive (e.g., light, pH, temperature)		
Alignment	Random		
	Aligned		
	Near-field electrospinning		
	3D structures (e.g., layer-by-layer, electrospinning on 3D templates, 3D printing and electrospinning hybrid)		

Table 1 lists the classification of electrospun nanofibers which vary widely in composition, structure, functionalization, and alignment. Compositionally, they include polymeric fibers (both natural and synthetic biodegradable), carbon fibers, and composites that integrate metal/metal oxides, carbon-based nanomaterials, drugs, bioceramics, dyes, and antimicrobial or antioxidant agents, as well as purely ceramic and metallic fibers.[33–37] Structurally, nanofibers can form monolithic, hollow, island-like, co-axial (core-shell), Janus, beads-in-fiber, multi-axial, porous, necklace-like, multichannel, helical, and "shish-kebap" shapes.[9,38] Functionalization often involves surface modifications, such as chemical groups, nanoparticles, or active molecules, and some fibers are stimuli-responsive, reacting to light, pH, or temperature changes.[39–45]

1.1.3. Recent Innovations in Electrospinning Technology

Significant developments in electrospinning instrumentation have provided wide application areas in laboratory scale and industrial production. First, single-needle systems such as mono-axial and co-axial were developed. While mono-axial systems provide unidirectional fiber production, co-axial systems produce core-shell fibers by combining two polymer solutions. Then, multi-needle systems (e.g., tri-axial and multi-axial) were launched in line with industrial-scale production requirements. These systems provide high production capacities and the fabrication of more complex structures. In addition, innovative methods such as centrifugal or rotating jet,[46,47] 3D,[48] and portable electrospinning,[49] which can be applied in both single-needle and multi-needle systems, have been developed. Given the drawbacks of needle-based systems, such as needle clogging, lower throughput, and labor-intensive processes, needleless electrospinning systems stand out as an important development. Free surface roller and wire systems allow fibers to be collected directly on a surface or from a wire, providing faster and more efficient production processes. Briefly, a rotating cylinder partially immersed in a polymer solution spins against a biased rotating collector, with airflow maintained and two motors independently controlling their speeds.[50] Rutledge et al. studied the influence of solution properties, including concentration, surface tension, and viscosity, along with system parameters like electric field and rotation speed, on the productivity of the process, particularly during the phases of entrainment, de-wetting, and jetting.[51] After the advancement of free-surface electrospinning, bubble electrospinning emerged, which enables the collection of fibers using the bubble surface under an electric field, enhancing fiber alignment and morphology.[52] When the bubbles are combined with ultrasound electrospinning, it leads to rapid fluid flow and the formation of micro-jets. This synergy results in improved fiber morphology and uniformity.[53,54] Furthermore, corona electrospinning creates jets from a rotating circular electrode forming Taylor cones at the sharp edges.[55] Moreover, high-speed electrospinning integrates electrostatic forces with rapid rotational jetting and fiber stretching, providing large quantities and fast production opportunities, and significantly boosting fiber production rates.[56]

1.2. Advancements in Photodynamic Therapy

1.2.1. History

Photodynamic therapy (PDT) is a medical treatment approach that utilizes light-sensitive compounds, called photosensitizers (PS), and a specific wavelength of light to produce reactive oxygen species (ROS), which can destroy nearby targeted cells. The history of the PDT concept began in the late 19th century with the discovery of photodynamic action by Oscar Raab. He observed that certain dyes when exposed to light in the presence of oxygen, could kill microorganisms.[57,58] Around the same time, the Danish physician Niels Finsen, used phototherapy for treating Lupus Vulgaris (a skin form of tuberculosis) and was awarded the Nobel Prize for his contribution to the treatment of diseases in 1903. Von Tappeiner and A. Jesionek took PDT to another level by screening small fluorescent molecules to target skin tumors and initiated the first clinical use of PDT. In 1907, von Tappeiner and Jodlbauer completed the missing piece of the puzzle by identifying the requirement of molecular oxygen to observe a photodynamic effect. In the early 20th century, Friedrich Meyer-Betz conducted the first human application of PDT by testing it on himself. He injected a significant amount of haematoporphyrin into his skin to study its effects and toxicity. In 1942, Auler and Banzer used porphyrins as PS to investigate the distribution of injected porphyrins in tumors.[59] Later, in 1948, Figge and his co-workers demonstrated the nonselective nature of porphyrins, showing that they accumulate in both malignant and healthy cells.[60,61] Although interest in photodynamic therapy (PDT) declined until the mid-20th century, Schwartz and Lipson

rediscovered the potential of porphyrins.[62] Schwartz's work in purifying crude hematoporphyrin and identifying its active components reignited interest in PDT research.[63] Following this, Lipson revealed that the hematoporphyrin derivative, obtained by acetic acid-sulphuric acid treatment provided a higher tendency to localize in cancerous cells and the possibility for diagnosis through its fluorescence properties.[64,65] The modern era of PDT began in the 1970s with the pioneering work of Thomas Dougherty. His team developed Photofrin, the first FDA-approved PS for clinical use. Notably, they conducted the first successful clinical trials using PDT for skin cancer treatment in 25 patients.[66] These promising results motivated further research into applying PDT to other types of cancer such as esophageal,[67] lung,[68] and gastric carcinoma.[69] The critical milestone of PDT was the approval of Phorphrin for the treatment of bladder cancer by the Canadian Health Protection Branch in 1993.[62] This was followed by approvals from the FDA and other authorities, and its applications expanded to non-cancerous conditions such as age-related macular degeneration, skin disorders, and infectious diseases.[70] The focus on the development of the new PS for the treatment of both cancer and non-cancerous diseases has accelerated, leading to FDA approval of aminolevulinic acid (1999), Verteporfin (2000), Temoporfin (2001), and methyl aminolevulinate.[71] In recent decades, advancements in PS and light delivery technologies have significantly improved the efficacy and precision of PDT, making it an established treatment for various cancers and other medical conditions.

1.2.2. Mechanism of Photodynamic Action

Photodynamic treatment utilizes three components: light-activated compounds (PS), a specific wavelength of light, and molecular oxygen.[72–74] When these three components come together, the PS molecule absorbs light and is promoted from its ground singlet state (S_0) to an excited singlet state (S_1). Once an electron is in the excited singlet state (S_1), it can release its energy via vibrational relaxations, emission (called fluorescence), or undergo intersystem crossing to a long-lived excited triplet state (T_1). The intersystem crossing rate (triplet quantum yield) and stability (lifetime) are crucial for effective photodynamic action. When the excited triplet state PS ($^3PS^*$) interacts with a non-toxic molecular oxygen it can produce different types of ROS by following two main pathways. In the type-I mechanism, $^3PS^*$ reacts with nearby biomolecules (such as proteins or lipids) through an electron transfer, leading to the formation of a radical anion of PS ($^3PS^{\bullet -}$) which then interact with the molecular oxygen to produce highly reactive superoxide ($O_2^{\bullet -}$). The $O_2^{\bullet -}$ can exhibit cytotoxicity or depending on its environment undergoes redox reactions and produce other ROS including hydroxy radical ($OH^\bullet$) and hydrogen peroxide (H_2O_2). In some cases, the PS* transfers its energy to ground-state molecular oxygen (O_2), which naturally exists in a triplet state ($^3O_2$) and leads to the formation of highly reactive singlet oxygen ($^1O_2$) capable of damaging cellular components. The production of ROS in cells induces oxidative stress, which damages cellular membranes, proteins, and nucleic acids, ultimately leading to either apoptosis (programmed cell death) or necrosis (uncontrolled cell death).[75–80]

1.2.3. Challenges in Application of PDT

Although PDT has a history spanning more than a century, it has gained significant attention for treating various diseases, including cancer and infectious diseases, particularly with recent technological advancements. Compared to conventional methods, PDT offers numerous advantages, such as minimal invasiveness, localized treatment, and reduced systemic toxicity. However, several challenges still limit its broader translation into widespread clinical applications.[74,81,82]

The low tissue penetration depth of light: Treatment requires a high light intensity to achieve effective photodynamic action. Many studies have focused on developing new PSs that produce ROS when illuminated within the therapeutic window (600–900 nm).[83] While this approach is effective for surface tumors, skin disorders, and dental applications, the scattering and absorption of light in deeper tissues significantly reduce its efficacy.

Poor target selectivity of PSs: Although some PSs preferentially accumulate in target cells, their selectivity is often not absolute, which can lead to uptake by healthy tissues. Due to the "always on" nature of most PSs, they can generate ROS in the presence of light (even daylight), potentially causing damage to healthy tissues.

Low water solubility of PSs: The water solubility of PSs directly impacts the effectiveness of PDT treatment. Solubility issues can result in poor bioavailability, inefficient biodistribution, formulation challenges, and potential off-target toxicities.

High long-term sensitization of PSs: PSs must selectively accumulate in the targeted tissue and be cleared from the body after light application. In skin applications, with high susceptibility to daylight exposure, slow clearance of PSs may result in prolonged activity and toxicity to healthy cells.

To overcome the challenges mentioned above and enhance the photodynamic effect, numerous PSs have been modified with targeting units (cancer drugs, antibiotics, cationic small molecules) have been developed.[84,85] Additionally, interest in the design of activatable PSs, which are non-phototoxic in healthy cell environments but undergo chemical activation in response to specific biomarkers (e.g., enzyme, pH, or bio-thiols) to generate ROS upon light irradiation, has increased substantially.[86–88] Another important strategy for achieving highly selective and effective PDT is the development of carrier systems. In this approach, the encapsulation or incorporation of PSs in various nanocarriers (e.g., liposomes, nanoparticles, nanofibers, dendrimers, carbon-based nanomaterials, quantum dots, and metal-organic frameworks) enhances their water solubility, improves bioavailability, and allows for controlled release, thereby reducing toxicity to healthy tissues.[89,90] Among nanocarrier systems, electrospun nanofiber-based delivery materials have significantly advanced PDT.[91–93]

1.2.4. Synergistic Benefits of Electrospinning and PDT

Electrospinning offers a unique and versatile approach to fabricating nanofibers with distinct advantages for PDT applications. One of the key benefits of electrospun nanofibers is their ability to deliver localized therapeutic agents directly to targeted sites, which helps minimize off-target toxicity. The targeted drug

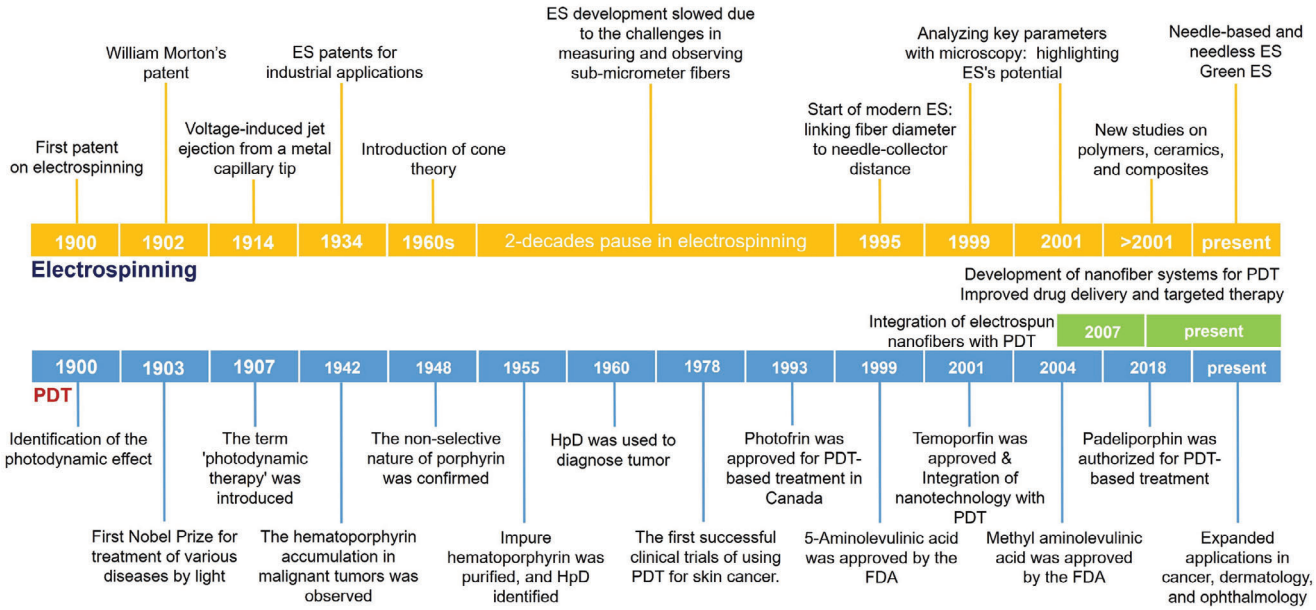

Figure 1. Timeline of electrospinning and PDT advancements.

delivery improves treatment effectiveness by localizing photosensitizers at the intended site, maximizing therapeutic efficacy. Furthermore, the high surface area-to-volume ratio of the nanofibers facilitates the efficient loading of therapeutic agents, making them ideal candidates for controlled and sustained release. The high surface area of nanofibers allows for greater interaction with light, facilitating better light absorption and subsequent ROS generation, which is essential for PDT.[94] The nanoscale size of the fibers also enables better penetration into tissue, ensuring more effective PDT performance at deeper tissue layers. The materials used in electrospinning are highly adaptable, and biocompatible and biodegradable that can be selected to ensure the safety of PDT applications. The flexible material selection allows for the fabrication of nanofibers that are safe and capable of breaking down naturally in the body after fulfilling their therapeutic function. This biodegradability is a significant advantage in reducing long-term toxicity and minimizing the need for invasive removal procedures. Electrospun nanofibers are also particularly well-suited for multi-drug delivery systems, as they can be loaded with a variety of therapeutic agents simultaneously, allowing for the combination of PDT with chemotherapy or photothermal therapy. Moreover, the morphology and mechanical flexibility of electrospun nanofibers can be tailored to suit specific therapeutic needs, such as optimizing fiber density, diameter, and surface texture to improve drug loading and release profiles.[95]

Figure 1 illustrates the integration of electrospinning with PDT, highlighting the development of nanofiber systems that improve drug delivery and targeted therapy. The use of electrospinning and PDT began to gain traction in 2007.[96–98] The discovery of new PSs, combined with advancements in nanotechnology, has accelerated ongoing PDT studies, many of which have received FDA approval. The synergistic effects of PDT with other therapeutic approaches, such as sonodynamic therapy (SDT) and antimicrobial peptides (AMPs), significantly enhance the overall therapeutic outcomes. Sonodynamic therapy involves the use of sonosensitizers that are activated by ultrasound to produce ROS, similar to PDT but with the advantage of deep tissue penetration due to ultrasound.[99] Sono-photodynamic therapy, a combination of PDT and SDT, can work synergistically by utilizing different types of energy (light and ultrasound) to activate their respective sensitizers, leading to a more comprehensive ROS generation and increased treatment efficacy, especially in deep or difficult-to-reach tissues. This combination can be particularly beneficial in cancer treatment, where both modalities can target tumor cells through different mechanisms, potentially overcoming the limitations of each therapy when used alone.[100] Similarly, the integration of antimicrobial peptides (AMPs) with PDT/PTT creates a potent strategy for combating infections. AMPs are naturally occurring molecules that have broad-spectrum antimicrobial properties and can disrupt the membranes of bacterial, fungal, or viral pathogens.[101] By combining PDT with AMPs, the therapeutic effect is amplified, as PDT-induced ROS can enhance the antimicrobial activity of AMPs, while AMPs can also help to target and neutralize resistant microorganisms that may survive PDT alone. This synergistic approach is particularly promising for treating infections in wound healing and chronic infections, where both tissue regeneration and pathogen eradication are needed.[102] The combination of electrospun nanofibers with multiple therapeutic strategies opens new possibilities for multimodal therapies, making the treatment more effective in overcoming complex medical challenges, including cancer, infections, and tissue regeneration.

The use of photoactive nanofibers for various PDT applications, including cancer, antimicrobial therapy, and wound healing is represented in **Figure 2**. PS-loaded nanofibers are activated by light exposure at a specific wavelength. This activation excites the PSs to a $^1PS^*$, then transitions to a T_1 via ISC to form an active $^3PS^*$. The interaction of $^3PS^*$ with O_2 leads to the formation of ROS such as $^1O_2$ and $O_2^{\bullet-}$. These ROS induce oxidative damage to cellular components, leading to apoptosis or necrosis in

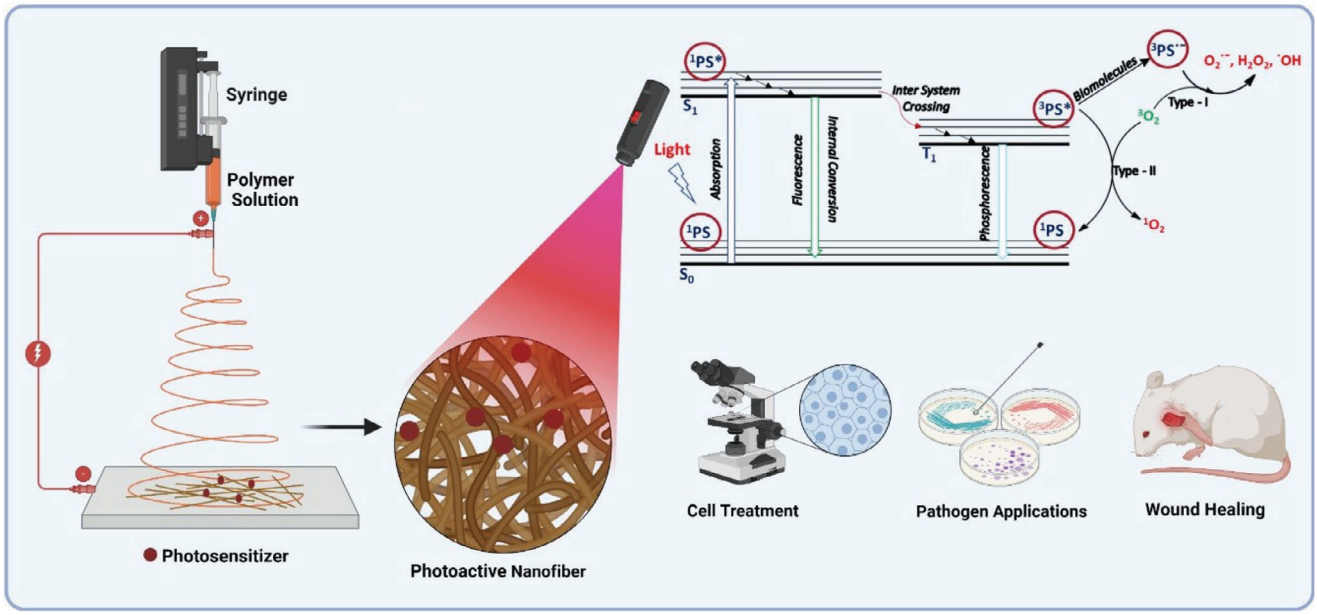

Figure 2. Schematic representation of electrospun photoactive nanofibers for PDT, generating ROSs under light exposure for applications in cancer treatment, pathogen applications, and wound healing. Figure created using BioRender.

targeted cells including cancer cells or pathogens. The nanofibers provide localized, sustained release of the PSs, enhancing their concentration at the target site and improving the efficacy of the PDT while minimizing damage to surrounding healthy tissues.

2. Classification of Photosensitizer-Loaded Electrospun Nanofibers

Electrospun nanofibers used in PDT can be classified based on several criteria related to PSs, including composition, loading capacity, functionality, application type, and the specific type of PSs employed.

In terms of composition, nanofibers can be fabricated from natural polymers, such as alginate, chitosan, and gelatin, which offer biocompatibility and biodegradability, or from synthetic polymers like poly (*ϵ*-caprolactone) (PCL), poly(lactic-co-glycolic acid) (PLGA), and polyvinyl alcohol (PVA), which provide enhanced stability and controlled release properties. The loading capacity of these nanofibers can be categorized as single PS-loaded, containing one type of PS for PDT, or multi-PS-loaded, which enables the combination of various PSs or therapeutic agents, including chemotherapy or photothermal agents.

Functionally, electrospun nanofibers can be designed to incorporate PSs with targeting moieties that enhance selectivity toward cancer cells, or they can be engineered to respond to specific stimuli, such as pH changes or light activation, allowing for the controlled release of PSs. In terms of application, these nanofibers can be utilized in wound dressings that integrate PSs for infection prevention, as implantable devices that release PSs directly to tumor sites, or in injectable systems that facilitate minimally invasive delivery of PSs. They can also serve in tissue engineering scaffolds that release PSs, enhancing PDT efficacy while supporting tissue regeneration.

Lastly, based on the type of PSs, electrospun nanofibers can be categorized according to their mechanism of action, including conventional PSs (e.g., chlorine, porphyrins) and new-generation PSs designed for specific conditions, optimizing their therapeutic effectiveness in PDT. In this review, we investigate electrospun nanofibers according to the type of PSs, primarily focusing on organic and inorganic PSs.

2.1. Organic Photosensitizers in Electrospun Nanofibers

Recently, the use of electrospun nanofibers as carrier systems in PDT has increased significantly. **Table 2** presents a summary of organic PSs incorporated into electrospun nanofibers, highlighting various agent/nanoparticle types, the specific electrospinning conditions employed, and the potential applications of these materials. The first example of incorporating a photoactive agent (fullerenes) into electrospun nanofibers was demonstrated by Stoilova et al. in 2007.[96] Fullerenes, particularly C_{60} and its derivatives, are highly promising PSs due to their unique structure and photophysical properties. However, their poor solubility in aqueous environments limits their bioavailability and applicability in biological systems. To address this, Stoilova grafted fullerenes onto amino-terminated polyethylene glycol (H_2N-PEG) by mixing the components under either homogeneous or heterogeneous conditions. They then successfully demonstrated the electrospinning of C_{60}-conjugated PEG with a biocompatible polymer, PCL, resulting in micro- and nanoscale fibers. Another application of fullerenes was demonstrated by Jiang and Le, who copolymerized fullerene with *N*-vinylpyrrolidone (VP) through radical polymerization. This copolymer exhibited phototoxicity against HeLa cells and mouse osteogenic sarcoma cells under light irradiation (500–600 nm; 60 mW cm^{-2}; 30 min).[103] The electrospinning of the copolymer with PVP resulted in

Table 2. Overview of organic photosensitizers used in electrospun nanofibers.

Materials Name	Electrospinning Conditions (Polymer/Solvent/Parameters)	Photosensitizer/Light Conditions	Cell Type	Target Species	Ref
H_xC_{60}(NHPEG)$_x$/PCL	PCL Chloroform 30kV/1.0mL min^{-1}	C_{60} ⩾600 nm 130 min	THP-1	*C. albicans*	[96]
Purpurin-18 loaded PLLA	PLLA Chloroform/Acetone 15kV/15cm/0.7mL h^{-1}	Purpurin-18 Laser, 702 nm	SMMC 7721, ECA 109	–	[98]
PVP/C_{60}–N-vinylpyrrolidone	C_{60}/VP THF 28kV/1.0mL min^{-1}	C_{60} Halogen lamp, 500-600 nm 60 mW/cm^2, 30 min	Lm8	–	[103]
PAN-Por$^{(+)}$	PAN DMF 15kV/15cm/0.75mL h^{-1}	Por$^{(+)}$ Halogen lamp, 400-700 nm 65±5 mW/cm^2, 30 min	Vero, A549, HAd-5	*S.aureus, VREfm, Acinetobacter baumannii, Klebsiella pneumoni, E. coli.*	[104]
TCPP@PLLA/PEO	PLLA/PEO DCM 8.5kV/15cm/1mL h^{-1}	TCPP Laser, 532 nm 100 mW/cm^2, 30 min	HeLa	–	[105]
PCN-224 NPs@PCL	PCL Chloroform-DMF 23kV/15cm 0.9mL h^{-1}	Por-based MOFs Laser, 630 nm 100 mW/cm^2, 10 min	L929	*S. aureus, E. coli*	[106]
PCS/TMP/TMPNPs	PU/PCEC/CS DMF 16 - 18 kV/20cm/1.0mL h^{-1}	Meso-tetrakis Por Laser, 635 nm 100 mW/cm^2, 0.5 min	HFFF2	*S. aureus, E. coli*	[107]
MPN@Zein-PpIX	Zein Ethanol -	PpIX 620-630 nm 30 min	L929	*S. aureus, E.coli*	[108]
Pc@Ag-SiO_2	PVP Ethanol 12kV/16cm/2.0mL h^{-1}	Pc Quartz lamp, 670±20 nm ∼10 mW/cm^2, 30 min	–	*S. aureus*	[110]
ZnTTQPc functionalized PA	Polyamide Formic acid/Acetic acid -	ZnTTQPc Quartz lamp, 670±40 nm 30 min	–	–	[111]
PS-loaded CS	CS/PEO Acetic Acid 80kV/15cm	Sulfonated AlPc LED, 675 nm 100 mW/cm^2, 30 min	MC3T3-E1, T-47D	–	[112]
PS-loaded CS	CS/PEO Acetic Acid 80kV/15cm	Sulfonated AlPc LED, 675 nm 8 mW/cm^2, 10 min	–	*S. aureus*	[113]
SiPc-PVA-CS	PVA/CS DMF 15-25kV/0.6-1.2mL min^{-1}	SiPc(COOH)$_4$ LED, 660±24 nm 70 mW/cm^2, 15 min	–	*Bacillus subtilis, E. coli*	[114]
CA/MB	CA Aceton/Water 12kV/0.5mL h^{-1}	MB Neon tube, 400-700 nm 180 min	–	*S. aureus*	[115]
PCL-MB, PH-MB, PM-MB	PCL block copolymers Water 20kV/0.3mL h^{-1}	MB Halogen lamp, 525-800 nm 5-10 mW/cm^2, 60 min	L929	*S. aureus, E. coli*	[117]
Z/PCL@MSNF@MB	Zein/PCL Chloroform/DMF 22kV/15cm/0.9mL h^{-1}	MB 660 nm 3.2 mW/cm^2, 20 min	L929	*S. aureus and E. coli*	[118]
UCNP/SM-PVDF	PVDF DMF/Acetone 22kV/15cm/8.4µL min^{-1}	MB Laser, 980 nm 2.5 W/cm^2, 5 min	L929	*S. aureus and E. coli*	[119]
UCNPs@Curcumin	PCL/PVP 10kV/10cm	Curcumin Laser, 808 nm 20 min	–	*MRSA and E.coli*	[120]
UCNPs@hypericin/PCL/PVP	PCL/PVP Acetone 10kV/10cm	Hypericin Laser, 808 nm 0.5 W/cm^2, 20 min	–	*MRSA*	[121]
RBiEPNs	PAN DMF 15kV/13cm/0.6mL h^{-1}	RB 380-780 nm 60 min	–	*Bacillus subtilis, E.coli*	[122]
RB@ZIF-8@PCL	PCL 22kV/15cm/15µL min^{-1}	RB Visible lamp, 515±5 nm 1.8 mW/cm^2, 30 min	–	*S. aureus, E. coli*	[123]
RB/CAR-loaded fibers	HPMC/Eudragit L100-55 HFIP/Ethanol 20kV/18cm/0.2 and 0.6mL h^{-1}	RB LED, 521 nm 3.3 mW/cm^2, 20 min	Caco-2, HDF	–	[124]
F-127/PCL/AgNPs/CUR	PCL/F-127 Chloroform 23kV/15cm/1.0mL h^{-1}	Curcumin LED, 450 nm 17.2 mW/cm^2, 15 min	–	*C. albicans*	[125]
PLA.NF.ICG.CUR	PLA Chloroform/Methanol 15kV/1.0mL h^{-1}	ICG and curcumin LED, 457 nm	L929	*S. aureus, E. coli*	[126]
PLA.NF.ICG	PLA Chloroform/DMF/EtoAc 20-60kV/22cm	ICG Laser, 810 nm ∼640 mW/cm^2, 30 min	L929	*S. saprophyticus, E. coli, S.aureus*	[127]
ICG/chitosan/PVA	PVA/CS Acetic acid 15kV/12cm/0.4mL h^{-1}	ICG Laser, 781 nm 500 mW/cm^2, 4 min	–	*MRSA, MRPA*	[128]
MoS_2-IR780-loaded fibers	PVA Water 14kV/15cm/1.0mL h^{-1}	IR780 Laser, 808 nm 1.5 W/cm^2, 10 min	NIH-3T3	*S. aureus, E.coli*	[129]
MNPs-enhanced NNHs	PCL 12kV/0.5-1.0mL h^{-1}	Melanin UV, 315-400 nm 2 min	BJ, A375	*S. aureus, E. coli*	[130]
MNP-PVA	PVA Water 18 kV/12cm/0.2mL h^{-1}	Melanin LED, 395-400 nm 3.4 mW/cm^2, 5 min	L929	*E. coli*	[131]
PVA–TBO	PVA Water 15kV/12cm/0.2mL h^{-1}	TBO NPs LED, 460 nm 0.1 W/cm^2, 60-120 min	–	*Bacillus subtilis, E. coli*	[132]
ACM-fibers	PCL HFIP 16kV/12cm/0.1mL min^{-1}	Ce6 Laser, 660 nm 5 mW/cm^2, 30 min	Eca-109	–	[133]
Ce6-fibers and CM-fibers	PCL HFIP	Ce6 Laser, 660 nm 5 mW/cm^2, 30 min	Eca-109 VX2	–	[134]
PAN-CQDs NFs	PAN DMF 11.7 kV/15cm/0.7mL h^{-1}	CQDs Xenon lamp, ⩾420 nm 275 mW/cm^2, 90 min	L929	*S. aureus, E. coli, P.aeruginosa*	[135]
hCQDs/PCL	PCL Chloroform/Methanol 9-25kV/13cm/1.0mL h^{-1}	hCQDs 470 nm 60 min	–	*K. pneumoniae L.monocytogenes*	[136]
PBAT/PLA/ZnPc	PBAT/PLA Chloroform/DMF 18-25kV/12cm/0.5mL h^{-1}	ZnPc	–	–	[137]
PLA-HA	PLA DMF/DCM 15-20kV/10-11cm/1.0mL h^{-1}	HA Laser, 470 nm 100 mW/cm^2, 30 min	L929	*C. auris*	[138]
Cur@PLGA-NPs	PLGA Chloroform/DMF 20kV/20cm/2.0mL h^{-1}	Curcumin Laser, 450 10 nm 1.6 mW/cm^2, 5 min	Vero	*SARS-CoV-2*	[139]
IMQ-PCL	PCL HFIP 10-25kV/13-19cm/0.01-2.0mL h^{-1}	Imiquimod	NIH-3T3, MCF-7 BCRC, SAS	–	[140]

Macromolecular Materials and Engineering Open Access
www.mame-journal.de

micro- and nanoscale fibers, with fiber diameters varying depending on the monomer concentrations used.

Porphyrins have also attracted significant interest in developing photoactive surface/textile materials in combination with electrospinning. Stanley et al. prepared a cationic porphyrin derivative embedded into nonwoven textile material, polyacrylonitrile (PAN) nanofibers (PAN-Por$^{(+)}$), for antimicrobial PDT uses.[104] The produced nanofiber offered a larger surface area and PS loading thus higher PDT efficacy was reached under light irradiation (400–700 nm; 65±5 mW cm^{-2};30 min) compared to cellulose-based materials. Ma et al. obtained a photoactive membrane by electrospinning of increasing amounts of 5,10,15,20-tetrakis (4-carboxyphenyl) porphin (TCPP) in poly(l-lactic) acid (PLLA)/polyethylene oxide (PEO) solution. The presence of PEO improved the hydrophilicity of the membrane and allowed the controlled release of uniformly dispersed PS.[105] In another study, Zhang et al. encapsulated TCPP into the zirconium-based metal-organic framework (PCN-224), then co-electrospun it with PCL to obtain antimicrobial membranes activated by light irradiation (630 nm; 100 mW cm^{-2}; 30 min).[106] To inhibit bacterial infections on cutaneous wounds during the healing period, Saghebasl et al. reported on the polyurethane (PU)/PCL–PEO–PCL/chitosan nanofibrous mat, which incorporates a cationic PS known as *meso*-tetrakis (*N*-methyl pyridinium-4-yl) porphyrin tetratosylate (TMP) salt. Furthermore, TMP-loaded chitosan tripolyphosphate nanoparticles were introduced into the composite nanofibrous mat, enhancing drug delivery.[107] To improve the biocompatibility, stability, and selectivity of protoporphyrin IX (PpIX), Zhou et al. conjugated PpIX to zein through EDC–NHS chemistry with %2.4 conjugation ratio then electrospun it to form nanofiber membrane. The hydrophobic surface of the membrane was coated with tannic acid and Fe^{3+} ions to construct the metallic polyphenol network (MPN) which provides hydrophilicity to the final photoactive membrane structure (MPN@Zein-PpIX). Importantly, MPN@Zein-PpIX enables the destruction of target cells under a light source over photodynamic (620–630 nm; 30 min) and photothermal (808 nm; 0.5 W cm^{-2}; 10 min) therapy.[108]

Phthalocyanines (PCs) are macrocyclic chromophores bearing absorbance and fluorescence features within the therapeutic window.[109] Binding a diamagnetic element (e.g., Zn, Al, Si) to the cavity of PC changes its electron transfer abilities, stabilizes triplet state electron, and enhances $^1O_2$ quantum yield.[110] Incorporation of PCs into nano-fiber structures enhanced their biocompatibility, stability and targetability. Goethals et al. investigated the effect of pre- or post-functionalization of polyamide nanofibers with (4)-tetra[2-thioquinoline]phthalocyaninato zinc(II) (ZnTTQPc) on photodynamic action for water sanitization. They observed only post-functionalization ensured PS localization on nanofibers' surface and produced $^1O_2$ under red light irradiation (670±40 nm; 30 min).[111] On the other hand, de S. Rossin et al. demonstrated the importance of fiber material to achieve PDT action. In their work, electrospinning of commercially available ZnPCs with poly(butylene adipate-co-terephthalate) (PBAT)/poly(lactic acid) (PLA) blend did not significantly diminish the $^1O_2$ production. The photoactive character of ZnPCs was also enhanced by coating them with gold nanoparticles[97] or silver nanoparticles decorated silica particles[110] which were electrospun with PMMA or PVP, respectively. The antimicrobial and anticancer photodynamic activity of nanofibers produced by electrospinning of Photosens, a mixture of sulfonated aluminum PCs, with chitosan (CS)/PEO studied by Severyukhina et al.[112,113] An interesting study presented by Galstyan and Strokov revealed the importance of the concentration ratio between PS (SiPc(COOH)$_4$) and polymers. They electrospun PVA-PS or PVA-CS-PS mixture with varying CS and PS ratios and obtained red light (660±24 nm; 70 mW cm^{-2}; 15 min) activatable five different membranes bearing homogenous morphologies. Based on antimicrobial activity studies, higher CS amounts provided a better photodynamic effect than high PS loadings.[114]

Besides the above-mentioned PSs, purpurin, phenothiazine, chlorin, xanthene, curcumin, and ICG-based photoactive molecules have also frequently been used to develop nanofiber-based platforms for both antimicrobial and anticancer purposes. Loading purpurin 18 into the PLLA nanofibers is one of the early applications of photoactive membranes. The introduction of purpurin 18 did not affect the fiber morphology and demonstrated significant killing performances under laser irradiation (702 nm; 10 mW cm^{-2}).[98] Czapka et al. fabricated a methylene blue (MB)-loaded CS nanofiber that exhibited antibacterial and antibiofilm properties.[115] A core-sheath nanofiber design was developed using thermoplastic polyurethane (TPU) as the core and zwitterionic and cross-linkable polysulfobetaine copolymer as the sheath unit. The MB-loaded core-sheath nanofiber has the potential to mimic skin due to its improved mechanical properties.[116] In another study, Chang and Chen synthesized a zwitterionic nanofibrous mat containing poly(2-methacryloxyloxyethyl phosphorylcholine) and PCL block co-polymers loaded with MB-bearing anti-biofouling and antimicrobial capability under light irradiation (525–800 nm; 5–10 mW cm^{-2}; 60 min).[117] The high-water absorption and retention capacity, and slow drug release profile make it an important candidate for long-term photoactive materials for wound dressing. Sun et al. demonstrated that MB-loaded mesoporous silica nanoparticles can demonstrate enhanced aPDT activity that is incorporated into the zein-PCL nanofiber matrix (Z/PCL@MSNF@MB). Additionally, the use of a highly fluorinated silica source (trichloro (1H, 1H, 2H, 2H-heptadecafluorodecyl) silane) provided an extra surface hydrophobicity and gained the nanofiber material a bacteria-repellent capacity.[118] Upconversion nanoparticles (UCNPs), composed of NaYF$_4$:Yb/Er/Gd, coated with MB-loaded silica nanoparticles displayed a good PDT activity under illumination of near-infrared (NIR) light (980 nm; 2.5 W cm^{-2}; 5 min). The upconversion luminescence bands of Yb^{3+} and Er^{3+} overlap with the absorption of MB and co-doping Gd^{3+} increases the upconversion efficiency. Electrospinning of PVDF/UCNPs and PVDF provided almost identical nanofibrous structures without any alteration.[119] Similar strategy utilized by Liu et al.UCNPs (NaYF$_4$:Yb/Tm@NaYF$_4$:Nd) were coated with curcumin and embedded core-shell NaYF$_4$:Yb/Tm@NaYF$_4$:Nd@curcumin into PCL/PVP fibers. In this study, with the aid of in situ electrospinning, better morphology was obtained and good wettability on different surfaces enhanced the effect of PDT.[120]

The technological developments contribute positively to the use of PDT in treatment in outdoor and point-of-care applications. Zhang et al. demonstrated the use of a portable

electrospinning device that is simply powered by a battery and allows the electrospinning of nanofibers directly onto the wound area. In this strategy, UCNPs ($NaYF_4$:Yb/Er@$NaYF_4$:Nd)-coated with hypericin embedded into PCL/PVP polymer mixture and electrospun onto the wound. UCNPs both prevented the leakage of PS to the wound due to larger particle size and activated the hypericin at a longer excitation wavelength (808 nm; 0.5 W cm^{-2}; 20 min). Additionally, precise deposition of the nanofiber prevents the harmful effect of PDT on healthy cells by allowing the delivery of ROS through eluting holes and accelerating wound healing.[121]

The effect of ionic strength and pH of application media was investigated by Dong et al. Membranes prepared from the electrospinning of PAN with an increasing concentration of Rose Bengal (RB) were subjected to the release test at different ionic strengths and pH values. The ionic strength did not show any influence but significant effects on PS release thus PDT activity was observed with varying pH of the media. To achieve controlled release and uniform surface distribution.[122] Qian et al. encapsulated RB into the zeolite imidazole framework-8 (ZIF-8) and co-electrospin with biodegradable PCL. The RB@ZIF-8 undergoes hydrolysis and slowly releases photoactive compounds.[123] RB was also used to enhance the activity of anticancer agent (carmofur) loaded into nanofiber structure consisting of Eudragit L100-55 shell (pH-sensitive) and hydroxypropyl methylcellulose (HPMC).[124] Braga et al. aimed to observe the synergistic effect of the combination of AgNPs bearing antimicrobial properties and curcumin with PDT activity embedded into F-127/PCL polymeric matrix (F-127/PCL/AgNPs/CUR) for the treatment of fungal infections.[125]

An interesting study by Gutberlet et al. reports the use of two photoactive compounds (ICG and Cur) embedded in a poly(D,L-lactide) (PLA) nanofiber matrix obtained through single-needle electrospinning for both photothermal and photodynamic inactivation of bacteria.[126] Irradiation of ICG with a NIR light source (810 nm; 500 mW cm^{-2}; 30 min) led to an increase in the temperature of the surrounding media and triggered the effective release of curcumin from the nanofiber membrane. Using a second light source (450 nm) suitable for curcumin allowed the generation of $^1O_2$ to provide photodynamic destruction of the targeted cells in combination with PTT. aPDT activity of ICG-loaded PLA nanofiber mesh (PLA.NF.ICG) against Gram (+) and Gram (–) bacteria was confirmed by Preis et al.[127] Upon irradiation of electrospun nanofibers under NIR light, the temperature increased within a few minutes and stayed high while released ICG generating ROS to destroy target cells. Similarly, the ICG-encapsulated CS/PVA composite nanofiber revealed significant photodynamic activity for wound healing applications. The liquid absorption capacity of the nanofibers was modified by incorporating various combinations of CS and PVA. The water absorption rate of nanofibers increases from 169% to 210% in 240 min when the PVA concentration is increased from 5% to 7%. This is due to the formation of intramolecular hydrogen bonds.[128]

Another important example of dual-mode therapy was demonstrated by Zhang et al. The nanofibers were obtained from electrostatically interacted MoS_2-IR780 nanocomposite which was embedded into the PVA/LA (α-Lipoic acid) polymer matrix. The mechanistic studies revealed that increased temperature enhanced the permeability of the bacteria membrane and allowed to achieve better PDT activity.[129] The drug delivery and PDT potential of monolithic and core-shell PCL nanofibers containing melanin nanoparticles (MNPs), ampicillin, or a combination of both were investigated by Kabay et al.[130] MNPs exhibited promising PDT activity (under UV-A irradiation; 315–400 nm; 2 min) and diminished the burst release of ampicillin. Switching polymer matrix to PVA and using single and coaxial nozzles allowed to obtain photoactive nanofibers with blend and core-sheath structures.[131] Besides known PSs, Jiang et al. synthesized a benzo[c]-1,2,5-oxadiazole-based nanoparticles bearing PDT activity under light illumination (460 nm; 0.1 W cm^{-2}; 60–120 min)[132] and embedded into PVA matrix to fabricate photoactive wound dressing material.

An important feature of nanofiber mats is their potential to be used as coating materials. Encapsulating PSs into the membrane structure allows photoactive surfaces and implants to be generated. Xiao et al. synthesized chlorin e6 (Ce6) conjugated albumin as a template for MnO_2 growth that enables the production of O_2 in cancerous cells under hypoxic conditions. The albumin–Ce6–MnO_2 system electrospun with PCL and poly(p-dioxanone) to obtain biodegradable stents used to treat oesophageal cancer.[133] In another study, they fabricated nanofiber stent initially electrospinning Ce6 with PLA, then post-modifying fiber surface for in situ MnO_2 mineralization. Besides its ability to generate O_2, MnO_2 coating protected non-tumor sites from laser irradiation and slowed the Ce6 release.[134]

Besides organic small molecules, carbon quantum dots (CQDs) providing high stability, biocompatibility, and low toxicity, large and functionalizable surface areas, and tunable optical properties are promising photosensitizers for PDT applications. Nie et al. synthesized CQDs from citric acid and 1,5-diaminonaphthalene by solvothermal method, mixed with PAN matrix and electrospun to form photoactive nanofibers without any effect on morphology.[135] In another example, hydrophobic CQDs were synthesized and electrospun with varying concentrations of PCL.[136] Each PCL ratio requires voltage optimization to prevent the formation of beads and obtain a uniform fiber structure. Additionally, CQDs required blue light (>420 nm) to produce ROS in both studies.

2.2. Inorganic Photosensitizers in Electrospun Nanofibers

The interest in inorganic nanomaterials has garnered significant attention in PDT/PTT applications due to their outstanding optical, electrical, and surface properties.[141] These materials offer high stability, tunable and enhanced absorption and emission characteristics, targetability based on various mechanisms (i.e., EPR), and multifunctional usability. **Table 3** provides an overview of inorganic PSs utilized in electrospun nanofibers. TiO_2 is highly interested in PDT applications due to its adjustable photophysical properties and low toxicity.

Sun et al. developed a photoactive material synthesized by coating UCNPs ($NaYF_4$:Yb,Tm nanorods) with TiO_2 (for PDT) which was then doped with graphene oxide (GO) (for PTT) to generate both ROS and heat.[142] The fabrication of uniform nanofiber material is achieved by electrospinning nanoparticles in PVDF. To achieve an effective and safe synergistic treatment,

Table 3. Overview of inorganic photosensitizers used in electrospun nanofibers.

Materials Name	Electrospinning Conditions (Polymer/Solvent/Parameters)	Photosensitizer/ Light Conditions	Cell Type	Target Species	Ref
UTG-PVDF	PVDF DMF/acetone 22kV/15cm/0.5mL h^{-1}	TiO_2 Laser, 980 nm 2.5 mW/cm^2, 5 min	L929	*S. aureus, E. coli*	[142]
Ce-N-TiO_2 loaded PLA	PLA DCM/DMF 20kV/20cm/1.0mL h^{-1}	TiO_2 Xenon lamp, >400nm 2 mW/cm^2, 30 min	L929	*S. aureus, E. coli*	[143]
MZ-8/PLA	PLA DCM 20–30 kV/15-20cm/1.0–2.0mL h^{-1}	ZIF-8 Laser, 808 nm 1.5 W/cm^2, 5 min	Hela, MCF-7	*MRSA, E. coli*	[144]
CS/PEO-CuSe	CS/PEO Acetic acid/Water 15kV/10µL min^{-1}	CuSe Laser, 1064 nm 0.8 W/cm^2, 20 min	L929	*MRSA, E. coli*	[145]
mPCL-Cu_2O	PCL/PANI DMF/DCM 12kV/20cm/0.05mm min^{-1}	Cu_2O LED, 520 nm 0.2 W/cm^2, 25 min	NIH-3T3	*S. aureus, E. coli*	[146]

UCPNs transfer NIR energy (>400 nm; 2 mW cm^{-2}; 30 min) to TiO_2 and GO via the FRET mechanism, which increases the temperature of the membrane and enhances the activity of produced ROS. PDT/PTT properties of Ti-based materials were also enhanced by doping with other elements or encapsulating in carrier systems. Doping cerium nitrogen to TiO_2 decreased the bandgap between the valence and conduction band caused a red shift on the absorption spectrum and elevated its catalytic activity to generate ROS.[143] Electrospinning of PLA matrix containing Ce-N-TiO_2 nanoparticles produced non-uniform nanofibers with reduced fiber diameter and bead-like structures. The deviation of the morphology of nanofibers from pure PLA can be attributed to the large amount of the Ce-N-TiO_2 nanoparticles that may weaken the homogeneity and spinnability of the polymer matrix. Zhang et al. developed a nano-assembly (MZ-8) prepared by in situ encapsulation of titanium carbide (MXene) into ZIF-8. The electrospun nanofibers, composed of MZ-8 and PLA, displayed remarkable PDT/PTT performance against living organisms under laser irradiation (808 nm; 1.5 W cm^{-2}; 5 min).[144] Zhao et al. demonstrated the use of a Re(I)-Gd(III) complex (Re-Gd) as a PS that is embedded into PVP fibers (Re-Gd@PVP). The rationale for the Re-Gd complex design relied on combining a photodynamically active Re(I) complex with a Gd(III) complex that enables its ligands to generate a stable excited T1 state via spin-orbit coupling effect. The stability of the T1 state enhances the probability of collisions between T1 and $^3O_2$. Additionally, immobilization of Re-Gd into PVP nanofiber provided extra stability and elongated excited state lifetime, preventing energy loss.[147] Electrospun mats are also important skeletons for nanoparticle systems acting as chemotherapeutic and photoactive materials. In another study, Cu_2O nanocubes were synthesized and incorporated into PLA electrospun mats. The designed platform demonstrated significant photodynamic performance under green light irradiation (520 nm; 0.2 W cm^{-2}; 25 min) to eradicate gram-positive and negative strains. Moreover, the release of Cu^{2+} ions provides an additional therapeutic effect on the antimicrobial performance of electrospun mats under dark conditions.[146]

Most of the applications of PDT in clinics rely on the activation of PS by a light at the therapeutic window. However, new materials with strong absorption properties have developed to obtain better tissue penetration and minimize potential side effects of light at high irradiation power. Yang et al. synthesized CS nanofiber embedded with CuSe NPs that can be directly deposited onto the bleeding region after surgery for rapid hemostasis and kill the target organism under NIR-II light irradiation (1064 nm; 0.8 W cm^{-2}; 20 min).[145]

3. Applications of Electrospun Nanofiber in PDT

3.1. PDT for Cancer Treatment

Extensive research continues to focus on cancer treatment, the deadliest disease impacting humanity. Traditional approaches, such as surgery, chemotherapy, and radiotherapy, remain common. However, as scientific advancements push forward, novel treatments such as immunotherapy, gene therapy, PDT, and thermal treatment have emerged.[148] PDT is a relatively new, non-invasive therapeutic technique against various diseases, including cancer. This treatment relies on generating ROS in the affected area, which helps to eliminate cancer cells.[149] Electrospun nanofibers, often combined with other materials such as films, sponges, or 3D-printed scaffolds, offer a versatile platform for cancer treatment. These fibers exhibit unique characteristics, including a large surface area, high capacity for drug loading, controlled release, and ease of modification, making them cost-effective for therapeutic applications.[148,150] Incorporating PSs into electrospun fibers enhances their potential in drug delivery and cancer treatment strategies. The difficulty in the treatment of cancer is the penetration of the effective therapeutic agent, particularly in solid tumors with extensive extracellular matrix.

Hybrid nanomaterials with enhanced potential for cancer treatment have gained significant attention. The composite electrospun nanofibers can selectively enter tumor tissue and be absorbed by cancer cells due to the nature of the active compounds.[151] Electrospun nanofibers commonly utilize active compounds (PSs), which can be selectively taken up by tumor tissues and activated by light to produce ROS that destroys cancer cells. For instance, Wu et al. used electrospun PLLA nanofibers containing purpurin 18 and applied to the human hepatocellular carcinoma (SMMC-7721) and the human oesophageal cancer cell line (Eca-109). Both are attached to and spread across the surface of the PLLA/purpurin 18 nanofibers, highlighting their excellent biocompatibility and lack of toxicity. MTT assays demonstrated that cancer cells were effectively destroyed after PDT treatment following exposure to 702 nm laser light. Furthermore, following irradiation, a significant reduction in the survival rates of both cell lines was observed, confirming that these cells could be effectively eliminated through PDT. Interestingly, in the absence of irradiation, the survival rate of the Eca-109 cells was notably low.[98] Moreover, when the human tongue squamous carcinoma cell line (HSC-3) was incubated with the electrosprayed PLGA-ALA nanoparticles and subsequently irradiated with 635 nm light at 500 mW for 2 min, cell death rates of 40–70% were observed.

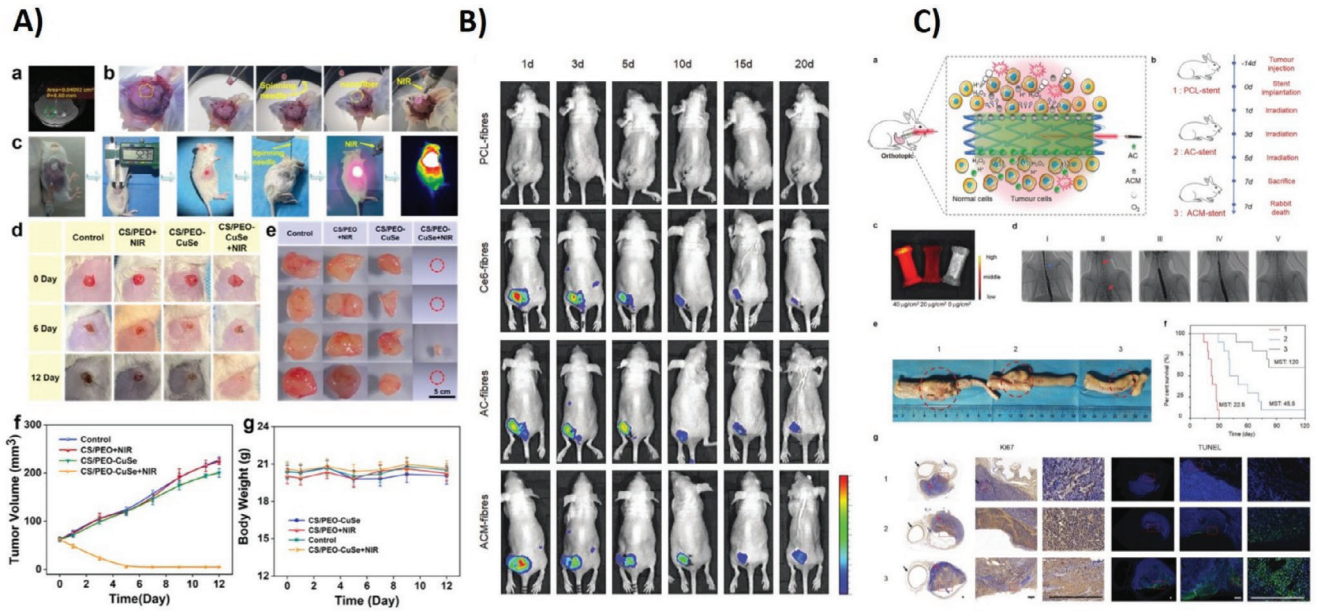

Figure 3. A) The simultaneous achievement of in vivo hemostasis, prevention of tumor recurrence, and analysis of wound repair, including MRI images of glioblastoma in tumor-bearing mice, a flowchart of the in vivo hemostasis process, the procedure for subcutaneous tumor treatment, and the recovery status of the tumor. Reproduced with permission.[145] Copyright 2023, Springer. B) In vivo evaluation of tumor duration and hypoxic relief using albumin-Ce6-MnO_2 (ACM) fibers in mice models, C) A schematic of the PDT process and photographs of tumor-bearing nude mice 14 days post-treatment, tumor growth curves, tumor weights from different groups at 14 days, body weight measurements over the same period, and CC3- and Ki-67-stained tumor slices collected 24 h after light irradiation. Reproduced with permission.[133] Copyright 2019, Wiley.

ALA facilitates the production of PpIX, a rapidly accumulating and highly effective PS in cancer cells.[152]

Electrospinning was used to synthesize CS/PEO nanofibers containing sulfonated aluminum PCs. The PCs, which were physically adsorbed, were initially released as the nanofibers swelled. A slower, sustained release occurred as a result of the degradation of the nanofiber matrix. Upon exposure to 675 nm laser irradiation, the metabolic activity of human mammary gland (T-47D) cancer cells treated with the scaffold was significantly inhibited, with no signs of recovery. Additionally, non-cancerous murine osteoblasts (MC3T3-E1) were less affected by irradiation[112] CS/PEO nanofibers have been combined with green synthesized CuSe nanoparticles. The obtained CS/PEO-CuSe composite nanofibers effectively induced cell apoptosis in malignant glioblastoma cells (U87 MG) while also demonstrating biocompatibility in fibroblast cells (L929).[145] (**Figure 3A**)

In another study, Lin et al. developed nanofibrous membranes composed of imiquimod and PCL (IMQ-PCL) for potential use in melanoma therapy. The IMQ-containing fibers caused a reduction of up to 10% in melanoma cell viability. The PDT activity of the membranes was investigated using mouse embryo fibroblast cell line (NIH-3T3), ER-positive human breast cancer cells (MCF-7), human malignant melanoma cells (BCRC), and human oral squamous cell carcinoma(SAS) cells.[140] Similarly, Kabay et al. reported that PCL/MNPs nanofibers are biocompatible with fibroblast cells, whereas induce up to 34% cell death in malignant melanoma cells upon UV-A irradiation.[130]

PS-loaded nanofibers have also proven to be a highly effective method for coating stents, enhancing their ability to treat tumors. For example, the performance of a drug-releasing stent coated with electrospun fibers containing albumin-Ce6-MnO_2 nanoparticles was tested in an orthotopic rabbit model of oesophageal cancer (Eca-109). The fiber-coated stents generated oxygen in response to tumor-produced H_2O_2, helping to mitigate the hypoxic microenvironment of the tumors. The oxygen production by the nanoparticles improved the effectiveness of PDT and increased animal survival rates, showing promise as an efficient strategy to target and eliminate localized solid tumors.[133] (Figure 3B,C) The same group of authors demonstrated the impact of stents coated with electrospun PCL fibers containing Ce6–MnO_2 on ECA-109 cells, highlighting their potential for future therapeutic applications.[134]

The advantageous combination of RB and carmofur in electrosprayed Janus particles exhibited non-toxicity to human dermal fibroblasts in the absence of light while inducing nearly complete cell death in human lung cancer (A549) cells following LED light exposure at 521 nm.[153] Similarly, Li et al. designed core-shell nanofibers by incorporating RB and carmofur. The cytotoxic effects of these nanofibers on human colon cancer (Caco-2) cells under light irradiation were investigated, showing significantly higher toxicity compared to non-cancerous human dermal fibroblast cells.[124] A PS-containing perfluorophenyl azide and *N*-hydroxysuccinimide (PFPA-NHS) were utilized to functionalize biomolecules on the surface of electrospun PCL scaffolds. When applied to the Caco-2 cells, promising results were observed.[154]

Suarez et al. developed PCL/Alginate and PCL/Gelatin nanofibers loaded with tamoxifen citrate and curcumin. They evaluated the cytotoxic effects on MCF-7 and PBMC cells. Their findings revealed that PCL–TMX nanofibers were highly toxic to both cell types, whereas PCL–Cur nanofibers exhibited lower toxicity.[155] Liu et al. created glycosylated Aza-BODIPY (LMBP)

and J-aggregate nanofibers. LMBP was able to selectively target human hepatocellular carcinoma (HepG2 cells), where it subsequently self-assembled into intracellular J-aggregate nanovesicles and nanofibers through supramolecular interactions. The study demonstrated that these J-aggregate structures generated $O_2^{\bullet-}$ via photoinduced electron transfer, facilitating efficient PDT. Additionally, the intracellular nanofibers disrupted HepG2 cell membranes and acted synergistically with PDT, resulting in potent tumor suppression in vivo.[156]

Systems combining electrospun nanofibers with PDT have proven effective not only in vitro but also in diverse in vivo experimental models. This approach provides a powerful method for inducing cell death in cancer therapies while significantly enhancing the proliferation and repair of healthy cells in wound tissues, leading to faster and more successful healing. Given its high efficiency and adaptability in cancer treatment, biocompatibility, and wound healing, this technology is expected to become increasingly significant in the future.

3.2. PDT for Antimicrobial and wound Healing Applications

3.2.1. Nanofiber-based PDT Systems for Bacterial Infections

Given the significant problem of bacterial resistance, the high incidence rates, and the diverse range of pathogens, researchers have increasingly focused on both aPDT and antimicrobial nanofibers, as well as their combined use. Upon closer inspection, it becomes evident that certain species of bacteria have evolved to become more suited for living on human skin as commensals.[157] Consequently, these bacteria have been the subject of increasing research due to their increased propensity to produce endogenous or exogenous skin diseases.[158] A variety of polymers and PSs have been studied for the eradication of *Staphylococcus aureus* and *Escherichia coli*, which poses a contagious risk due to their carriage in various skin conditions or lesions, in addition to possessing the features above.[159,160] The frequent isolation of these microorganisms, along with their representation of two distinct cell walls, indicates that they are commonly examined together in studies.

MB is a non-porphyrin compound that has been recognized for its antimicrobial properties for decades.[161] The high capacity of ROS production has made it one of the most frequently chosen structures in PDT investigations.[162] Recent data has provided additional insight into the toxicity of MB; nevertheless, as this toxicity results from internal usage, the molecule can still be used externally, and its approval for the treatment of periodontitis and dental caries has even been made possible.[115] MB-loaded zwitterionic nanofibrous mat demonstrated excellent water absorption and retention, cytocompatibility, and anti-biofouling properties, preventing L929 cell adhesion. Also, these systems have been effective in wound infections caused by both *E. coli* and *S. aureus*. Although the remarkable water absorption and retention capabilities are essential for wound healing and non-cytotoxic effects, it was noted that PS was released from its content over an extended duration. Consequently, it was determined that this nanofiber, which is believed to have a longer- the lasting effect could be appropriate for long-term use as a result of the anti-biofouling property of the relevant mat structure. After being exposed to medium-level light (100 W m^{-2}), it exhibited antibacterial activity comparable to those of kanamycin and tetracycline.[117] A promising approach for treating wounds by eliminating these two bacteria is the use of PVDF/UCNPs nanofiber structures upon activation by a NIR light (5 min.). This non-cytotoxic nanofiber membrane destroys both *S. aureus* (%94.5) and *E. coli* (%93.2), also has the benefit of having antibacterial action that lasts for up to four cycles.[119] In another study, Z/PCL@MSNF@MB fibrous composite acted as a ROS generator to enhance their antimicrobial properties. The fluorinated MSN tended to be enriched on the nanofiber's surface due to its low surface energy, which greatly increased the production of ROS. The composite membrane then showed impressive aPDT activity against *S. aureus* and *E. coli* upon exposure to visible light (660 nm). Both fluorinated and non-fluorinated structures have been shown to significantly limit bacterial viability (to less than %20). On the other hand, fluorinated membranes exhibit much higher efficiency than that of non-fluorinated samples (The viability of both bacteria has decreased to 3% or lower). This condition is believed to be caused by the enhanced hydrophobicity of the membrane surface in addition to the elevated aPDT activity.[118]

The prevalent application of MB as a PS and its FDA approval have heightened interest in utilizing various dyes for similar purposes. A recent study demonstrated that ICG and curcumin-loaded PLA electrospun nanofibers exhibit significant antibacterial properties and fibroblast cell proliferation. The initial step in these nanofibers involved the activation of ICG with infrared light (IR) and the regulation of curcumin release. Bacterial death was initiated by the blue light-stimulated system following the IR application, as a result of the ROS production of curcumin. This dual application significantly reduced the bacterial viability of *E. coli* and *Staphylococcus saprophyticus* subsp. bovis, a Gram-positive bacterium that causes infection in mucous membranes (~4.4 log10, 99.996%). As compared to nanofibers loaded with a single PS and stimulated with a single wavelength of light, it was found that the dual effect obtained was more effective. Furthermore, the synergistic impact achieved through this dual treatment proved effective in eradicating bacteria within the biofilm, with a reduction of 4.3 log10 (99.995%).[126] Likewise, an additional study employing the synergistic effects of photothermal and photodynamic mechanisms utilized the photosensitizer molecule PpIX in combination with a metal polyphenol network. The electrospun MPN@Zein-PpIX nanofiber derived from zein effectively exhibited bacterial suppression. A metal polyphenol network, formed by the chelation of the phenolic hydroxyl groups of MPN-polyphenols with metal ions, was established on the nanofiber membrane to achieve a synergistic effect. This structure, which is easily synthesized and biocompatible, integrates the photothermal effect with the photodynamic effect conferred by PpIX as a PS. The acquired nanofiber exhibited superior efficacy compared to systems utilizing PSs and photothermal agents independently, achieving bacterial reductions of 97.5% for *S.aureus* and 66.8% for *E.coli* respectively. The MPN@Zein-PpIX membrane exhibits no potential cytotoxicity toward L929 cells.[108] (**Figure 4A**)

In another study, the investigation of the efficacy of electrospun PAN nanofibers loaded with varying concentrations of RB revealed that the release profile remained unaffected by the ionic strength of the medium, although exhibited variations based on

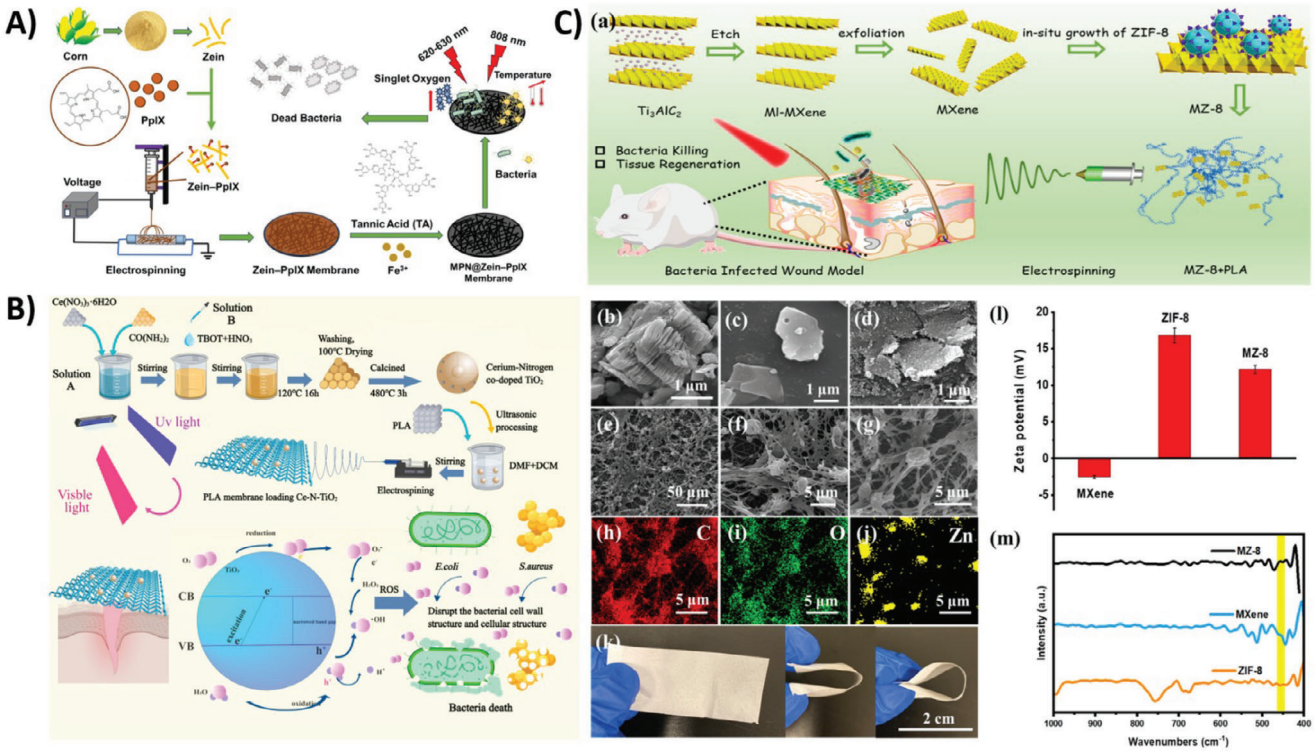

Figure 4. A) Schematic representation of the development of the MPN@Zein-PpIX membrane designed for integrated PTT and PDT.Reproduced with permission.[108] Copyright 2024, American Chemical Society. B) Diagram of the synthesis process for Ce-N-TiO_2 NPs loaded electrospun PLA membranes, illustrating the photocatalytic reaction under visible light to generate ROS for effective eradication of bacteria. Reproduced under the terms of the Creative Commons CC BY 4.0 license. [143] Copyright 2024, Frontiers. C) Preparation and characterization of the MZ-8/PLA electrospun membrane, including SEM images, elemental mapping, optical photograph, zeta potential, and FTIR spectra analysis. Reproduced with permission.[144] Copyright 2021, Elsevier.

pH levels. It was established that a greater quantity of dye was released at a higher pH level. The system exposed to white light produced an instantaneous and detrimental effect on *Bacillus subtilis* within a brief duration of 30 s, resulting in a 5.76 log reduction. Nevertheless, extended irrigation durations were necessary for *E. coli* a log reduction of 5.94 was achieved following 40 minutes of light exposure.[122]

Recent studies have shown that metal-based nanoparticles can be used as PSs. Due to the advantages of metal nanoparticles such as narrow size and shape and long activity period, expansion in this field has been booming in recent years.[163] A study conducted by Lv et al. is an example of a metal nanoparticle-based aPDT system that was conducted to eradicate *S. aureus* and *E. coli* in wound dressings. Following visible light irradiation, the PLA electrospun membrane containing 0.2Ce-N-TiO_2 NPs demonstrated remarkable bactericidal activity against *S. aureus* and *E. coli*, while preserving outstanding biocompatibility and slightly low cytotoxicity. *S. aureus* and *E. coli* were effectively eradicated, and the survival rates of both types of bacteria were substantially lower than %20 after 30 minutes of irradiation.[143] (Figure 4B) Similarly, a membrane fabricated using electrospinning, consisting of MXene, ZIF-8, and PLA (MZ-8/PLA), exhibited increased photothermal and photodynamic therapeutic efficacy against infections and tumors, regulated by NIR light. The inhibition rates against *E. coli* and methicillin-resistant *S. aureus* (MRSA) surpass 99.0%, and these fibers have demonstrated efficacy in the healing of MRSA-infected wounds during in vivo studies.[144] (Figure 4C) Another metal-based nanoparticle, CuSe, which exhibits high absorption in the (NIR-II) window, has been embedded in CS and PEO composite nanofibers. Despite the primary objective of fabricating this nanofiber structure to facilitate PDT-mediated tumor suppression, nanofibers exhibited *E. coli* and *S. aureus* inhibition properties.[145]

The critical significance of the investigation of the effects of nanofiber aPDT studies on a broader and diverse pathogen panel may extend beyond human-associated infections to include animal health and food safety. Alongside the traditionally examined pathogens, the assessment of efficacy against resistant *Klebsiella pneumoniae*, commonly found on surfaces like catheters or intubation materials, and against *Listeria monocytogenes*, a foodborne pathogen that induces severe conditions in neonates or immunocompromised individuals, could mitigate the microbiological problems related to medical devices or food products. The antibacterial efficacy of electrospun nanofibers composed of PCL and hydrophobic carbon quantum dots (hCQDs) was demonstrated in Ghosal et al. Nanofibers have been found to generate singlet oxygen when exposed to blue light at 470 nm and are proficient in eradicating Gram-positive (*S. aureus, L. monocytogenes*) and Gram-negative (*E. coli, K. pneumoniae*) bacteria. While the nanofibers showed efficacy against all species examined in the

study, the antibacterial activity against *S. aureus, E. coli*, and *L. monocytogenes* was particularly noticeable. Nonetheless, the approach proved to be less efficacious for *K.pneumoniae* than for others. Although the study did not specify the reasons, the fact that all *K.pneumoniae* are encapsulated and that this structure impedes the entry of nearly all substances into the cell should not be disregarded.[136]

Antibiotic resistance is not the only obstacle to effective wound infection treatment. Concerning wound care and prevention, biofilm development and antiseptic/ disinfectant ineffectiveness are also major issues.[164] A multi-drug resistant pathogen, *Pseudomonas aeruginosa*, is skilled at decreasing its sensitivity to all treatments, particularly through the reduction of membrane permeability.[165] Given the substantial number of studies in which *P. aeruginosa* has been tolerant to antiseptics or disinfectant agents, it is expected that approaches acting through different mechanisms, like aPDT, will have great potential in treating or preventing a broad range of *P. aeruginosa* infections such as pressure ulcers, burns, and wound infections.[166] Studies have looked into the efficacy of ICG-loaded CS and PVA nanofibers in preventing and eliminating carbapenem (the last resort antibiotic group with the broadest spectrum) resistant *P. aeruginosa* strain.[128] Although an effective antibacterial effect was observed in vitro against this resistant strain, the release of PS led to a favorable outcome in vivo of preventing the infection on the wound surface. Preis et al. employed needle-free electrospinning to develop PLA.NF.ICG nanofibers as a wound dressing. This nanofiber network demonstrated strong biocompatibility, as evidenced by the proliferation of mouse L929 cells, not only on the surface but also within the deeper layers of the material. Additionally, the dressing exhibited effective antimicrobial properties, particularly against such as *Staphylococcus saprophyticus, Escherichia coli*, and *Staphylococcus aureus*.[127]

In another study investigating the effectiveness of nanofiber-mediated aPDT for the eradication of this notorious bacterium, carbon quantum dots were used to eliminate the disadvantages of conventional PS such as poor water dispersibility, complex synthesis steps, difficulty of purification. Upon loading the carbon quantum dots into nanofiber-derived PAN powder via solvothermal synthesis, a reduction in *P. aeruginosa* strain of over 6 logs was seen upon light exposure for 1.5 h.[135]

Electrospun nanofibers represent an expanding area, applicable not only in wound dressings and drug delivery systems but also in textiles, owing to their advantageous characteristics, including many surface functional groups, elevated surface area to volume ratio, lightweight nature, and significant porosity.[167] Specifically in the hospital setting, using self-sterilizing materials can reduce the frequency and dissemination of nosocomial infections. This scenario can also inhibit the spreading of resistance markers among species. Stenly et al. investigated the antibacterial activity of PAN-Por$^{(+)}$ nanofibers against microorganisms from the ESKAPE pathogen family, including *S. aureus*, vancomycin-resistant *Enterococcus faecium*, *Acinetobacter baumannii, K. pneumoniae*, and *E. coli*. The generated nanofibers demonstrated a minimum of 5.8 log reduction in pathogens on the material surface of all examined bacteria following light illumination (30 min.; 65±5 mW cm^{-2}; 400–700 nm).[104]

3.2.2. Nanofiber-Based PDT Systems for Fungal Infections

Candida spp. are frequently isolated on skin infections, particularly in wounds.[168] While they are generally not regarded as a threat to healthy individuals, they can result in recurrent and challenging-to-treat infections due to predisposing factors.[169] There are, however, only a few types of antifungal drugs that can be used to treat fungus, and each one has drawbacks like major side effects, a restricted spectrum of antifungal activity, and resistance that makes them less useful in clinical settings.[170] Electrospun nanofibers appear to have the potential to offer rapid efficiency and simplified application for aPDT systems.[171] For instance, the surface property of PCL/AgNPs/CUR electrospun nanofibers was enhanced with F-127 surfactant, improving the hydrophilicity and thus cell adhesion, migration, and proliferation. The blue LED light irradiation of F-127/PCL/AgNPs/CUR nanofibers effectively eradicate *C. albicans* by facilitating substantial curcumin release and elevated $^1O_2$ induction at approximately pH 8, which reflects the wound pH.[125] *C. auris*, a recently identified fungal agent, is anticipated to provide a significant global problem due to its resistance profile and diagnostic challenges.[172] Acute or chronic skin infections caused by this pathogen can lead to invasive infections through systemic circulation, significantly increasing mortality rates.[173] To eradicate *C. auris*, PLA electrospun nanofibers are infused with hypocrellin A (HA), a pigment derived from natural sources (*Hypocrella bambusae*) that possess ROS generation capabilities has been proposed. PLA-HA nanofibers markedly diminished the number of pathogens in both the planktonic and biofilm models. Alongside its non-hemolytic nature and elevated biocompatibility, nanofibers must be particularly suitable for reuse. Furthermore, as demonstrated by in vivo tests, PLA-HA-aPDT may reduce inflammatory response and accelerate wound healing infected with *C. auris* while posing no obvious health risks.[138]

3.2.3. Nanofiber-Based PDT Systems for Viral Infections

The interest in employing aPDT for virus elimination has been increased by the scarcity of molecules that can be employed for antiviral purposes and their adverse effects.[174,175] Beyond the potential it holds solely for viral therapy, viral resistance to this approach has not yet been observed, as evidenced by antiviral aPDT investigations.[176] Viral structures are relatively straightforward and may comprise genetic material, a protein membrane, and a lipid envelope structure. Consequently, it is anticipated that the aPDT approach will have an impact on one or more of these three points.[177] While there is a lack of research specifically focused on identifying the mechanisms of action that are specific to viruses, it is established that PSs have been reported to exhibit DNA/RNA intercalation in studies.[176] Furthermore, some studies indicate that the generation of ROS has an impact on the lipid composition of enveloped viruses. Viruses often become active after entering the host cell through certain receptors. The distribution of these molecules within the body dictates tissue tropism, yet it is highly improbable that the nanofiber-aPDT combination will be utilized in therapy, particularly when considering respiratory-transmitted viruses.[178] However, the suppression of viral contamination in blood products is becoming

an increasingly essential method of application in this field.[179] The potential of curcumin-loaded PLGA nanoparticles, which were fabricated by electrospraying, has been demonstrated. The bioavailability of curcumin was increased while maintaining its original properties. This system, which is activated by blue light, has demonstrated a potent antiviral effect against the SARS-CoV-2 virus. In addition to not being toxic to cells, nanoparticles have also been shown to have no discernible effects on total plasma protein concentration, anti-A and/or anti-B antibody titers, or anticoagulation factors.[139] Due to the presence of certain favorable attributes the revealed nanofiber/nanoparticle system has the potential to provide high-potential products that can mitigate transfusion problems that may arise in blood products, particularly during the window period.

3.2.4. Nanofiber-Based aPDT Systems for Wound Healing

As the largest organ, the skin is the first barrier that protects the organs from environmental factors. Disruption of this barrier for various reasons may leave the internal organs vulnerable to various damages, especially infectious agents, and may also lead to disruption of the body's natural thermal balance.[180] Especially in the case of large and or chronic wounds, failure to properly perform wound care can lead to vital problems. Although it is a critical step to eliminate the infectious factors in the wound or prevent contamination with these factors, it is also necessary to provide different parameters for the wound to heal. Normal fibroblasts at the wound borders multiply and move in the direction of the wound site throughout the wound healing process. At the same time, they secrete matrix elements like collagen, elastin fibers, and polysaccharides, as well as fibrous tissue.[181] Wound healing is a complex biological process that involves four interrelated phases: hemostasis, inflammation, proliferation, and remodeling. For this intricate process, it is essential to develop biomaterials that can effectively mimic the native structure of the skin.

Advancements in technology, particularly in electrospinning, have significantly contributed to the development of bioactive dressings that are effective in treating both acute and chronic wounds.[148] Electrospun nanofibers possess properties that are highly conducive to wound healing, as their 3D architecture closely mimics the extracellular matrix (ECM) of the skin, supporting cell adhesion, survival, and proliferation during regeneration. A critical aspect of scaffold-based tissue regeneration is the ability to create an environment that mimics natural tissues, thereby supporting cellular growth and development. Cell behavior is frequently influenced by the ECM and bioactive factors.[150]

Intracellular structures are also very important, apart from the ECM, which provides support and structure to the cell outside the cell. The cytoskeleton, a complex network of protein fibers within cells, plays a crucial role in maintaining cell shape, enabling movement, and facilitating intracellular transport.[151]

Nanofiber scaffolds can be incorporated with antibiotics, metal and metal oxides, lysozymes, antimicrobial polymers, and peptides to effectively treat infected wounds and enhance antibacterial activity against bacterial and fungal pathogens.[182] Their ability to conform to wound areas, combined with the controlled release of therapeutic agents and PSs, plays a crucial role in promoting the wound-healing process.[94,183]

Electrospun fibers loaded with PSs demonstrate significant potential in wound treatment, as they can inhibit cell proliferation when exposed to laser irradiation. This approach has proven effective not only in preventing bacterial infections and biofilm formation but also in inhibiting cancer cell growth. Biofilms, often formed by bacterial species on tissue surfaces, create barriers that hinder granulation tissue development and reduce the effectiveness of antibiotics in reaching the wound bed, contributing to the progression of wounds into chronic, non-healing states. By targeting residual tumor cells, preventing bacterial invasion, and disrupting biofilms, these strategies enhance antibiotic efficacy, supporting wound healing and providing substantial benefits to both patients and the healthcare system.[112,181] Jiang et al. demonstrated that nanofibers designed for continuous wound protection under visible light exhibit excellent cytocompatibility with fibroblast cells known as NIH-3T3 and effectively inhibit biofilm formation when exposed to visible light.[132]

An ideal wound dressing should possess characteristics such as biocompatibility, biodegradability, breathability, water absorption, and dust resistance, along with strong antimicrobial properties. It should also be designed to prevent any damage to the tissue when removed.[184] Electrospun nanofiber structures are a promising alternative to traditional wound dressings. They can be designed to offer ideal conditions for wound healing, particularly by maintaining moisture levels, and their high surface area makes them well-suited for drug delivery. Additionally, the porous nature of these nanofibers can be tailored to block microorganisms from entering the wound while still allowing oxygen to flow through, promoting a cleaner and healthier healing environment.[185]

Many local or systemic factors can lead to impaired wound healing. Since systemic factors are characterized as a person's healing ability depending on individual characteristics, the potential of nanofiber structures on local factors related to wound healing.[186] Saghebasl et al. investigated the potential of a PCS nanofibrous mat with TMP as a wound dressing to cure a full-thickness excisional wound in both human fetal fibroblast cells (HFFF2) and a rat model.(**Figure 5A**) Compared to the rats without mats, the groups that received topically applied PC, PCS, PCS/TMP/TMPNPs mats had a greater and faster wound closure rate, as demonstrated by the data. There were, however, no significant differences between the nanofibers. Furthermore, the study evaluated the blood clot index (BCI) for predicting potential changes in the permeability of the wound dressing as a result of fibrin development over time. The best BCI performance was demonstrated by PCS/TMP/TMPNPs nanofiber mats, which is primarily caused by the positive charge of TMP. In this scenario, the system's permeability can be prevented by the formation of fibrin, which results in a reduction in blockage.[107,187] A biodegradable electrospun PCL matrix incorporating RB and ZIF-8 nanocrystals exhibited significant antibacterial effects against *S. aureus* and *E. coli*. Notably, the mat exhibited no hemolytic activity but enhanced wound healing by promoting bacterial eradication through ROS generated by visible light stimulation in a murine wound model.[123] (Figure 5B) Another PCL-based nanofiber was fabricated using porphyrinic metal–organic-frameworks for effective use as wound dressings

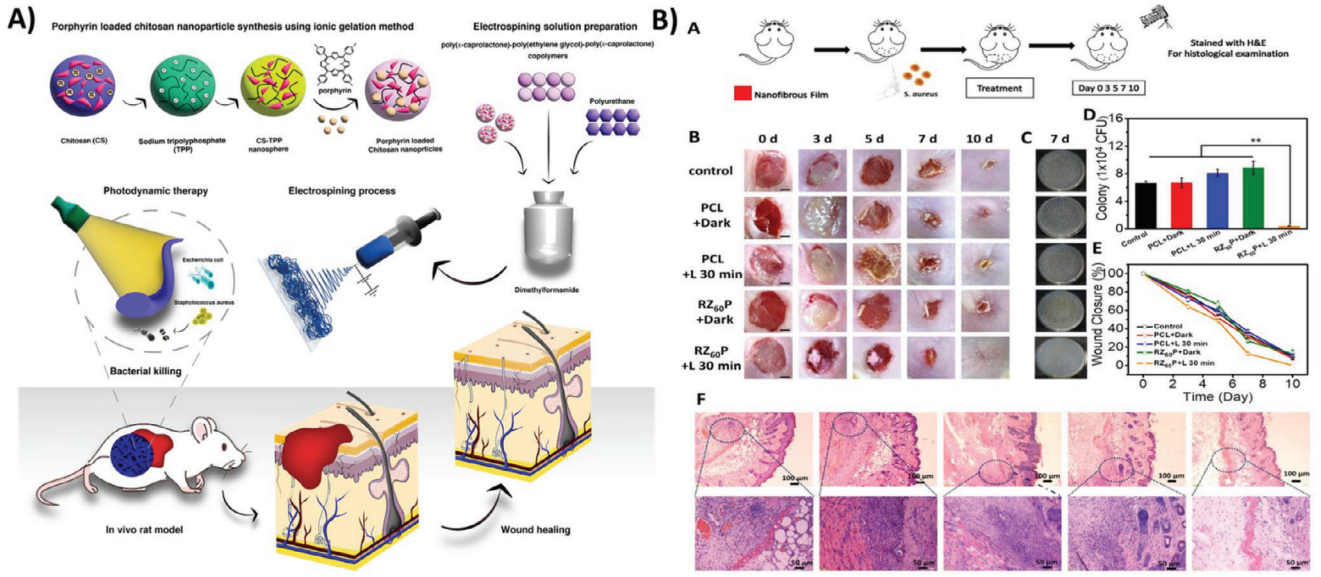

Figure 5. A) The photosensitivity and bactericidal effects of the polyurethane-based nanofibrous mat with porphyrin-loaded chitosan nanoparticles on skin tissue healing in a rat model. Reproduced under the terms of the CC BY-NC-ND 4.0 license.[107] Copyright 2023, BMC. B) Overview of the mice wound infection and treatment process using PCL/RB@ZIF-8 membranes, including photographs of wound healing progress, wound area measurements, *S. aureus* colony counts on LB agar after 7 days, and hematoxylin-eosin stained images of infected and treated skin tissues. Reproduced with permission.[123] Copyright 2020, Elsevier.

in L929 cultures.[106] Silver ions are commonly utilized for their antibacterial properties, however because of their toxicity and immunoinhibitory effects, safer metal substitutes are frequently required. Given its antimicrobial properties and its active involvement in biological processes related to wound healing, including angiogenesis, vascular growth, collagen deposition, and re-epithelialization, copper is the most promising alternative to silver. Zhao et al. used this characteristic to create a smart wound dressing by electrospun fibrous mats of modified PCL with photochemically active nanocrystalline cuprous oxide (Cu_2O). These biocompatible and nontoxic mats demonstrated over 99% suppression of *E. coli* and *S. aureus* after 25 min of light treatment. Because of their copper content, they were also uncontaminated by bacteria even when there was no light. Additionally, it is noteworthy that the scratch assay model utilizing NIH-3T3 cells showed considerable wound healing.[146]

PVA-based nanofibers have low toxicity, excellent biocompatibility, and mechanistic and permeability qualities, which make them useful for biodegradable wound dressings, mats, and filters.[188] It has been demonstrated that PVA-based electrospun nanofiber wound dressings, which use melanin nanoparticles as PSs and can be activated by UV light, are an effective option for eliminating pathogens and healing wounds. After being subjected to UV light for 30 s, the electrospun nanofibers–prepared in two distinct configurations as blended and core sheat–provided 41% and 32% suppression of *E. coli*, respectively. Comparing the wound closure capabilities of nanofibers containing solely PVA to the control groups, no discernible differences were identified, in the scratch assay (L929). Even in the absence of UV-A irradiation, the healing process was considerably accelerated by the addition of MNP to the nanofibers' composition, rising to 72% for the blended and 86% for the core-sheath nanofiber. It is also quite encouraging that the wound closure rate for core-sheath nanofibers rises to 99.2% when the experimental sets are exposed to a 30-second UV-A light irradiation.[131] Similarly, it was demonstrated that MRSA and meropenem-resistant *P. aeruginosa* had high resistivity properties, and ICG-loaded nanofibers made with a PVA-CS mixture have bactericidal capacity. Moreover, the nanofiber that emerges facilitates the wound healing process by absorbing exudate in addition to eliminating bacteria. By combining the bacterial eradication achieved by photodynamically stimulating the ICG with the increase in the exudate absorption capacity of the PVA-CS mixture, a more effective enhancement in the in vivo model was achieved. By the end of the 15 days, it was discovered that the application of the applicable wound cover had a favorable impact on several cellular markers linked to wound healing, in addition to a notable decrease in scarring in the ICG-CS PVA and light-containing group. It was discovered that there was a rise in CD31 glycoprotein expression, which was indicating of neovascularization. Likewise, it was believed that the decline in F4/80 expression secreted by mature macrophages signified a reduction in the activation of wound macrophages, and the immune system's impact on wound healing had diminished. As other immune system markers linked to wound infections, a decrease in the levels of interleukin-6 (IL-6) and tumor necrosis factor-α (TNF-α) was found to be a clear sign of wound healing.[128]

The mechanical characteristics of the wound dressing should be as close to the properties of human skin as achievable in addition to its role in pathogen-related and healing processes. Guo et al. developed MB-loaded zwitterionic TPU core-sheath nanofibrous membranes that mimic the extensibility of human skin, maintaining the wound dressing's properties throughout the healing and stretching process.[116] Similarly, in another study, researchers synthesized a novel co-electrospun cellulose acetate/TPU photodynamic helical fiber antibacterial membrane

by leveraging the mechanical advantages of TPU. After 20 min of daylight exposure, these nanofiber structures were able to inhibit *E. coli* and *S. aureus* by 99% or more by utilizing caffeic acid and phthaloyl phthalic acid photosensitizers. Additionally, under dark conditions, TDPA benzophenone may have preserved antimicrobial effects. The researchers additionally determined that the antibacterial efficacy of the nanofibers was not significantly diminished in the presence of light or under dark when they were reused after being washed.[189]

People with underlying causes typically have greater rates of persistent wound infections. Consequently, it is crucial to use immunocompetent animal models, particularly in in vivo research. As an instance, El-Khordagui et al.[190] demonstrated that *S. aureus* strains were effectively inhibited by PHB/PEG nanofibers loaded with MB. In the in vivo model, the group that received MB-NF light exhibited complete recovery. Additionally, the expression of VEGF mRNA–one of the cell profiling centers–increased in the study where the rise in epithelialization was demonstrated histopathologically. There was also a decrease in TNF expression, which is one of the immune system markers. It's interesting to note that although the study identified a phasic release kinetics, it also claimed that cationic PSs behaved similarly in this kinetics. Due to the wound environment's quick water absorption, 42% was released quickly within one hour, but the remaining 43% of discharges were steady for up to 7 days. Repeating the experiment with a constantly changing sample medium revealed considerably faster release kinetics, but it also demonstrated that drug release is directly dependent on the hydrodynamic conditions of the wound.

3.3. Challenges, Opportunities, and Future Directions

Nanofiber-based PDT systems provide versatile and effective solutions for managing bacterial, fungal, and viral infections, as well as promoting wound healing by enhancing antimicrobial activity and tissue repair. PDT has different material requirements and clinical applications in antibacterial and anticancer therapies because of its distinct biological targets and treatment goals. In antibacterial PDT, PSs must interact effectively with bacterial cell walls and biofilms. Cationic and hydrophobic PSs are generally favored, as they adhere to negatively charged bacterial surfaces and penetrate the membrane.[191–193] For neutral or anionic photosensitizers effective aPDT activity is possible by encapsulation of PSs into the cationic delivery vehicles such as nanofibers.[194] On the other hand, for anticancer treatment, the vast majority of PSs, when successfully delivered and PDT's other parameters (light and O_2) were fulfilled, have the potential to effectively destroy cancer cells. Additionally, as cancer induces hypoxic conditions, the preferred PS should provide high ROS generation ability in the presence of light at the therapeutic window (600–800 nm). Moreover, decorating PSs with targetting units such as anticancer drugs, antibiotics, peptides, etc. enhances the PDT efficacy for both treatments.[195] The mechanisms of action also differ: antibacterial PDT primarily causes oxidative damage to bacterial cell membranes, proteins, and nucleic acids, while anticancer PDT triggers apoptosis or necrosis by targeting intracellular structures like mitochondria and lysosomes, often activating an immune response.[196] Clinically, antibacterial PDT is effective in treating localized infections and antibiotic-resistant strains, with minimal side effects and lower risk of resistance development. However, it faces challenges in biofilm disruption. Future advancements in antibacterial PDT focus on portable devices and multifunctional PSs with anti-inflammatory properties, while anticancer PDT research emphasizes integrating PDT with other therapies and developing theranostic PSs for simultaneous diagnosis and treatment.

Furthermore, the clinical translation of electrospun nanofiber-based PDT systems requires careful consideration of their stability, scalability, and regulatory compliance. Stability is a critical factor, as photosensitizers embedded in nanofibers must maintain their functionality over extended periods without significant photobleaching, degradation, or leaching. Techniques such as encapsulation, the addition of stabilizing agents, and protective coatings have been explored to enhance the long-term stability and shelf-life of these materials.[197]Ensuring reproducible performance under various storage and application conditions is paramount for advancing these systems to clinical use.

Scalability presents another significant challenge, as transitioning from laboratory-scale electrospinning to industrial-scale production demands consistent batch-to-batch quality and optimization of parameters. This challenge is particularly relevant for PDT applications, where the uniformity and functional properties of nanofibers directly influence the therapeutic efficacy, including photosensitizer loading, release profiles, and light-mediated activation. Emerging technologies, such as needleless electrospinning, show promise in addressing these challenges, offering the potential for higher throughput while maintaining fiber uniformity. Other approaches, such as multi-jet electrospinning, rotary jet spinning, and free-surface electrospinning, enhance scalability by increasing production rates and simplifying processes. Techniques for fabricating 3D structures, including layer-by-layer electrospinning and dynamic collector systems, are also advancing, providing tailored architectures for PDT applications, including wound healing and antimicrobial treatments. Additionally, automation and real-time monitoring streamline production, ensuring uniform fiber properties and functional consistency at industrial scales.[198]

Clinical implementation of nanofiber-based PDT systems also necessitates robust preclinical and clinical studies to validate their efficacy and safety. While preclinical studies have shown encouraging results, translating these findings into clinical applications requires addressing biological variability and ensuring biocompatibility. Regulatory pathways for nanofiber-based PDT systems must adhere to stringent standards, such as those set by the Food and Drug Administration (FDA) and European Medicines Agency (EMA), to ensure safety and efficacy. There are FDA-approved electrospun-fiber-based medical devices used in different applications such as tissue engineering and dural defects repair.[132] Similarly, FDA-approved photosensitizers, such as Photofrin, Levulan, and Metvix, have demonstrated efficacy in clinical settings for treating cancer and certain skin conditions. Integrating these photosensitizers into electrospun nanofiber matrices not only holds promise for enhancing the performance of PDT but also facilitates a smoother regulatory process by utilizing existing safety and efficacy data.[91,199]

Although the use of PDT to treat various diseases, including cancer, infections, and skin disorders, has shown great promise,

another of the main limitations for clinical translations is the delivery of light to the targeted area. The low penetration depth of the light, even in the NIR region, restricts its applicability to treat many diseases. Each disease necessitates advanced light-delivery systems, such as fiber optics or interstitial light delivery, which must also be approved for efficacy and safety.[199] Economic and logistical factors also play a pivotal role in clinical translation. The cost-effectiveness of nanofiber-based PDT systems compared to conventional treatments needs thorough evaluation. Moreover, logistical aspects, including sterilization, storage, and transportation, must be streamlined to ensure widespread accessibility. Collaborations between academia, industry, and regulatory bodies are essential to address these challenges and facilitate the adoption of these systems in healthcare. Further research is needed to overcome existing limitations and explore multifunctional nanofibers that integrate diagnostic and therapeutic capabilities. By leveraging advancements in material science and promoting interdisciplinary collaborations, the full potential of electrospun nanofiber-based PDT systems can be unlocked, leading to significant breakthroughs in cancer therapy, antimicrobial treatments, and wound healing.

4. Conclusion

PS-loaded nanofibers represent a transformative approach in biomedical applications, providing targeted and localized therapies for cancer treatment, infection control, and wound healing. Among their numerous advantages, nanofibers offer high surface area, flexibility in drug loading, and excellent biocompatibility, which support cell proliferation and tissue regeneration. The fiber composition and porosity tunability allows for precise control over PS release, thereby enhancing treatment efficacy. However, challenges remain, particularly regarding limited light penetration in deeper tissues, which restricts PDT's efficacy to surface-level applications. The optimization of fiber parameters, such as PS loading, degradation rate, and mechanical properties, remains complex and highly application-specific. Despite these challenges, PS-loaded nanofibers are poised to become a vital tool in the future of medicine. Their ability to deliver localized therapies, control drug release, and enable selective activation minimizes side effects while enhancing therapeutic outcomes. Future research should prioritize the development of multifunctional nanofibers that combine PDT with other therapeutic modalities, improve biocompatibility, and advance wearable or implantable light-delivery systems. With ongoing innovations, PS-loaded nanofibers are expected to play a crucial role in personalized, minimally invasive medicine, offering safer and more effective treatments for complex conditions like cancer, chronic wounds, and infections.

Acknowledgements

M. U. would like to acknowledge funding from The Scientific & Technological Research Council of Türkiye (TUBITAK) through the 2247-D National Early Stage Researchers Program under Grant No. 121C212. A.E. and M.U. thank TUBITAK for the National Postdoctoral Research Fellowship Program under Grant No. 123C358. N.H. thanks the Scientific Research Projects Coordination Unit of İzmir Katip Çelebi University (Project no: 2024-TYL-FEBE-0023) for financial support.

Conflict of Interest

The authors declare no conflict of interest.

Keywords

electrospinning, nanocarrier, photoactive nanofiber, photodynamic therapy, photothermal therapy

Received: January 10, 2025
Published online: February 14, 2025

[1] Z.-M. Huang, Y.-Z. Zhang, M. Kotaki, S. Ramakrishna, *Compos. Sci. Technol.* **2003**, *63*, 2223.
[2] L. Rayleigh, *Proceedings of the London Mathematical Society* **1878**, *1*, 4.
[3] L. Rayleigh, *Proceedings of the Royal Society of London* **1879**, 71.
[4] J. F. Cooley, *United Kingdom Patent* **1900**, *6385*, 19.
[5] W. J. Morton, Method of dispersing fluids, **1902**, US Patent 705, 691.
[6] J. Zeleny, *Phys. Rev.* **1914**, *3*, 69.
[7] F. Anton, *Washington, DC: US Patent and Trademark Office* **1934**.
[8] G. I. Taylor, *Proceedings of the Royal Society of London. A. Mathematical and Physical Sciences* **1969**, *313*, 453.
[9] A. Keirouz, Z. Wang, V. S. Reddy, Z. K. Nagy, P. Vass, M. Buzgo, S. Ramakrishna, N. Radacsi, *Adv. Mater. Technol.* **2023**, *8*, 2201723.
[10] J. Doshi, D. Reneker, in *Proceedings of IEEE Industry Application Society 28th Annual Meeting*, IEEE, Ind Applicat Soc, **1993**, pp. 1698–1703.
[11] H. Fong, I. Chun, D. H. Reneker, *Polymer* **1999**, *40*, 4585.
[12] Z.-M. Huang, Y.-Z. Zhang, *Chem. J. Chin. Univ.-Chin.* **2005**, *26*, 968.
[13] C. Burger, B. S. Hsiao, B. Chu, *Annu. Rev. Mater. Res.* **2006**, *36*, 333.
[14] P. Li, Y. Liu, J. Yao, in *2010 International Conference on Information Technology and Scientific Management*, **2010**, pp. 326–328.
[15] A. Yarin, E. Zussman, *Polymer* **2004**, *45*, 2977.
[16] D. Sun, C. Chang, S. Li, L. Lin, *Nano Lett.* **2006**, *6*, 839.
[17] L. Chen, S. Mei, K. Fu, J. Zhou, *ACS nano* **2024**.
[18] T. Subbiah, G. S. Bhat, R. W. Tock, S. Parameswaran, S. S. Ramkumar, *J. Appl. Polym. Sci.* **2005**, *96*, 557.
[19] N. Horzum, E. Boyacı, A. E. Eroglu, T. Shahwan, M. M. Demir, *Biomacromolecules* **2010**, *11*, 3301.
[20] D. H. Reneker, A. L. Yarin, H. Fong, S. Koombhongse, *J. Appl. Phys.* **2000**, *87*, 4531.
[21] W. Zuo, M. Zhu, W. Yang, H. Yu, Y. Chen, Y. Zhang, *Polym. Eng. Sci.* **2005**, *45*, 704.
[22] S. Kailasa, M. S. B. Reddy, M. R. Maurya, B. G. Rani, K. V. Rao, K. K. Sadasivuni, *Macromol. Mater. Eng.* **2021**, *306*, 2100410.
[23] M. G. McKee, G. L. Wilkes, R. H. Colby, T. E. Long, *Macromolecules* **2004**, *37*, 1760.
[24] P. Gupta, C. Elkins, T. E. Long, G. L. Wilkes, *Polymer* **2005**, *46*, 4799.
[25] C. Cleeton, A. Keirouz, X. Chen, N. Radacsi, *ACS Biomater. Sci. Eng.* **2019**, *5*, 4183.
[26] M. Ahmadi Bonakdar, D. Rodrigue, *Macromol* **2024**, *4*, 58.
[27] M. M. Demir, B. Ozen, S. Ozcelik, *J. Phys. Chem. B* **2009**, *113*, 11568.
[28] M. M. Demir, N. Horzum, B. Ozen, S. Ozcelik, *J. Phys. Chem. B* **2013**, *117*, 10920.
[29] H. Hu, W. Jiang, F. Lan, X. Zeng, S. Ma, Y. Wu, Z. Gu, *Rsc Advances* **2013**, *3*, 879.
[30] W.-H. Han, M.-Q. Wang, J.-X. Yuan, C.-C. Hao, C.-J. Li, Y.-Z. Long, S. Ramakrishna, *Arabian J. Chem.* **2022**, *15*, 104193.
[31] S. De Vrieze, T. Van Camp, A. Nelvig, B. Hagström, P. Westbroek, K. De Clerck, *J. Mater. Sci.* **2009**, *44*, 1357.

[32] J. Pelipenko, J. Kristl, B. Janković, S. Baumgartner, P. Kocbek, *Int. J. Pharm.* **2013**, *456*, 125.
[33] N. Horzum, D. Taşçıoglu, S. Okur, M. M. Demir, *Talanta* **2011**, *85*, 1105.
[34] N. Horzum, R. Munoz-Espi, G. Glasser, M. M. Demir, K. Landfester, D. Crespy, *ACS Appl. Mater. Interfaces* **2012**, *4*, 6338.
[35] N. Horzum, D. Mete, E. Karakuş, M. Üçüncü, M. Emrullahoğlu, M. M. Demir, *ChemistrySelect* **2016**, *1*, 896.
[36] G. K. Özdemir, A. Bayram, V. Kılıç, N. Horzum, M. E. Solmaz, *Anal. Methods* **2017**, *9*, 579.
[37] M. H. Elhousseini, T. Isık, Ö. Kap, F. Verpoort, N. Horzum, *Appl. Surf. Sci.* **2020**, *514*, 145939.
[38] T. D. Nguyen, S. Roh, M. T. N. Nguyen, J. S. Lee, *Micromachines* **2023**, *14*, 2022.
[39] N. Horzum, T. Shahwan, O. Parlak, M. M. Demir, *Chem. Eng. J.* **2012**, *213*, 41.
[40] N. Horzum, M. M. Demir, M. Nairat, T. Shahwan, *RSC advances* **2013**, *3*, 7828.
[41] E. Boyacı, N. Horzum, A. Çağır, M. M. Demir, A. E. Eroğlu, *Rsc Advances* **2013**, *3*, 22261.
[42] G. Onak, M. Şen, N. Horzum, U. K. Ercan, Z. B. Yaralı, B. Garipcan, O. Karaman, *Sci. Rep.* **2018**, *8*, 17620.
[43] G. Atik, N. M. Kilic, N. Horzum, D. Odaci, S. Timur, *ACS Appl. Mater. Interfaces* **2023**, *15*, 24109.
[44] G. Evren, E. Er, E. E. Yalcinkaya, N. Horzum, D. Odaci, *Biosensors* **2023**, *13*, 673.
[45] F. R. Karaduman, S. Turk Culha, N. Horzum, *ACS Appl. Bio Mater.* **2024**, *7*, 5345.
[46] A. L. Andrady, D. S. Ensor, R. J. Newsome, *Electrospinning of fibers using a rotatable spray head*, **2006**, US Patent 7,134,857.
[47] R. Weitz, L. Harnau, S. Rauschenbach, M. Burghard, K. Kern, *Nano Lett.* **2008**, *8*, 1187.
[48] A. Keirouz, M. Chung, J. Kwon, G. Fortunato, N. Radacsi, *Wiley Interdiscip. Rev.: Nanomed. Nanobiotechnol.* **2020**, *12*, e1626.
[49] S.-C. Xu, C.-C. Qin, M. Yu, R.-H. Dong, X. Yan, H. Zhao, W.-P. Han, H.-D. Zhang, Y.-Z. Long, *Nanoscale* **2015**, *7*, 12351.
[50] O. Jirsak, F. Sanetrnik, D. Lukas, V. Kotek, L. Martinova, J. Chaloupek, *Method of nanofibres production from a polymer solution using electrostatic spinning and a device for carrying out the method*, **2009**, US Patent 7,585,437.
[51] Y. Shin, M. Hohman, M. Brenner, G. Rutledge, *Polymer* **2001**, *42*, 09955.
[52] Y. Liu, J.-H. He, J.-Y. Yu, *J. Phys.: Conf. Ser.* vol. *96*. IOP Publishing, **2008**, pp. 012001.
[53] H. J. Nieminen, I. Laidmäe, A. Salmi, T. Rauhala, T. Paulin, J. Heinämäki, E. Hæggström, *Sci. Rep.* **2018**, *8*, 4437.
[54] A. Korkjas, K. Laar, A. Salmi, J. Mäkinen, E. Hæggström, K. Kogermann, J. Heinämäki, I. Laidmäe, *J. Drug Delivery Sci. Technol.* **2022**, *78*, 103935.
[55] K. Molnár, Z. K. Nagy, G. Marosi, L. A. Meszaros, Hungarian patent p1200677, **2012**.
[56] Z. K. Nagy, A. Balogh, B. Démuth, H. Pataki, T. Vigh, B. Szabó, K. Molnár, B. T. Schmidt, P. Horák, G. Marosi, G. Verreck, I. V. Assche, M. E. Brewste, *Int. J. Pharm.* **2015**, *480*, 1.
[57] O. Raab, *Zeitschr Biol* **1900**, *39*, 524.
[58] V. TAPPEINER, *Dtsch. Arch. Klin. Med.* **1904**, *80*, 427.
[59] J.-C. Diels, L. Arissian, *Lasers: the power and precision of light*, John Wiley & Sons, Weinheim **2011**.
[60] F. H. Figge, G. S. Weiland, L. O. Manganiello, *Proceedings of the Society for Experimental Biology and Medicine* **1948**, *68*, 640.
[61] D. Rassmussen-Taxdal, G. E. Ward, F. H. Figge, *Cancer* **1955**, *8*, 78.
[62] T. J. Dougherty, C. J. Gomer, B. W. Henderson, G. Jori, D. Kessel, M. Korbelik, J. Moan, Q. Peng, *J. Nat. Cancer Inst.* **1998**, *90*, 889.
[63] S. Schwartz, K. Absolon, H. Vermund, *Univ Minn Med Bull* **1955**, *27*, 7.
[64] R. L. Lipson, E. J. Baldes, A. M. Olsen, *J. Thorac. Cardiovasc. Surg.* **1961**, *42*, 623.
[65] R. L. Lipson, E. J. Baldes, A. M. Olsen, *J. Nat. Cancer Inst.* **1961**, *26*, 1.
[66] D. TJ, *Cancer Res.* **1978**, *38*, 2628.
[67] J. S. McCaughan Jr, W. Hicks, L. Laufman, E. May, R. Roach, *Cancer* **1984**, *54*, 2905.
[68] O. J. Balchum, D. R. Doiron, G. C. Huth, *Las. Surg. Med.* **1984**, *4*, 13.
[69] Y. Hayata, H. Kato, H. Okitsu, M. Kawaguchi, C. Konaka, in *Seminars in Surgical Oncology*, vol. *1*, Wiley Online Library, Hoboken, NJ **1985**, pp. 1–11.
[70] D. E. Dolmans, D. Fukumura, R. K. Jain, *Nat. Rev. Cancer* **2003**, *3*, 380.
[71] A. M. Oluwajembola, W. D. Cleanclay, A. F. Onyia, B. N. Chikere, S. Zakari, E. Ndifreke, O. C. De Campos, *Results in Chemistry* **2024**, 101715.
[72] A. P. Castano, T. N. Demidova, M. R. Hamblin, *Photodiagn. Photodyn. Ther.* **2004**, *1*, 279.
[73] S. Kwiatkowski, B. Knap, D. Przystupski, J. Saczko, E. Kedzierska, K. Knap-Czop, J. Kotlińska, O. Michel, K. Kotowski, J. Kulbacka, *Biomed. Pharmacother.* **2018**, *106*, 1098.
[74] M. Klausen, M. Ucuncu, M. Bradley, *Molecules* **2020**, *25*, 5239.
[75] U. Muhammed, K. Erman, K. D. Eylem, S. Melike, D. Suay, E. Mustafa, *Org. Lett.* **2017**, *19*, 2522.
[76] S. Dartar, M. Ucuncu, E. Karakus, Y. Hou, J. Zhao, M. Emrullahoglu, *Chem. Commun.* **2021**, *57*, 6039.
[77] M. Przygoda, D. Bartusik-Aebisher, K. Dynarowicz, G. Cieślar, A. Kawczyk-Krupka, D. Aebisher, *Int. J. Mol. Sci.* **2023**, *24*, 16890.
[78] W. Jiang, M. Liang, Q. Lei, G. Li, S. Wu, *Cancers* **2023**, *15*, 585.
[79] P. Delcanale, S. Abbruzzetti, C. Viappiani, *La Rivista del Nuovo Cimento* **2022**, *45*, 407.
[80] P. S. Maharjan, H. K. Bhattarai, *J. Oncol.* **2022**, *2022*, 7211485.
[81] G. Gunaydin, M. E. Gedik, S. Ayan, *Front. Chem.* **2021**, *9*, 691697.
[82] Y. Allamyradov, J. ben Yosef, B. Annamuradov, M. Ateyeh, C. Street, H. Whipple, A. O. Er, *Photochem* **2024**, *4*, 434.
[83] A. N. Bashkatov, E. A. Genina, V. I. Kochubey, V. Tuchin, *J. Phys. D: Appl. Phys.* **2005**, *38*, 2543.
[84] J. Gao, H. Jiang, P. Chen, R. Zhang, N. Liu, *Bioorg. Chem.* **2023**, *136*, 106554.
[85] M. Ucuncu, B. Mills, S. Duncan, M. Staderini, K. Dhaliwal, M. Bradley, *Chem. Commun.* **2020**, *56*, 3757.
[86] M. Liu, C. Li, *ChemPlusChem* **2020**, *85*, 948.
[87] B. Yuan, H. Wang, J.-F. Xu, X. Zhang, *ACS Appl. Mater. Interfaces* **2020**, *12*, a26982.
[88] Z. Li, Z. Zhou, Y. Wang, J. Wang, L. Zhou, H.-B. Cheng, J. Yoon, *Coord. Chem. Rev.* **2023**, *493*, 215324.
[89] A. Qidwai, B. Nabi, S. Kotta, J. K. Narang, S. Baboota, J. Ali, *Photodiagn. Photodyn. Ther.* **2020**, *30*, 101782.
[90] N. W. Nkune, H. Abrahamse, *Int. J. Mol. Sci.* **2021**, *22*, 12549.
[91] H. Maleki, M. Doostan, S. Shojaei, M. Doostan, H. Stamatis, E. Gkantzou, A. Bonkdar, K. khoshnevisan, *J. Drug Delivery Sci. Technol.* **2023**, *82*, 104367.
[92] G. Pandey, S. Shah, V. Phatale, P. Khairnar, T. Kolipaka, P. Famta, N. Jain, D. A. Srinivasarao, A. Asthana, R. S. Raghuvanshi, S. Srivastava, *J. Drug Del. Sci. Technol.* **2023**, 105249.
[93] M. Babazadeh-Mamaqani, D. Razzaghi, H. Roghani-Mamaqani, A. Babaie, M. Rezaei, R. Hoogenboom, M. Salami-Kalajahi, *Prog. Mater. Sci.* **2024**, 101312.
[94] S. M. Costa, R. Fangueiro, D. P. Ferreira, *Macromol. Biosci.* **2022**, *22*, 2100512.
[95] G. Kuang, X. Lin, J. Li, W. Sun, Q. Zhang, Y. Zhao, *Chem. Eng. J.* **2024**, 151253.

[96] O. Stoilova, C. Jérôme, C. Detrembleur, A. Mouithys-Mickalad, N. Manolova, I. Rashkov, R. Jérôme, *Polymer* **2007**, *48*, 1835.
[97] S. Tombe, W. Chidawanyika, E. Antunes, G. Priniotakis, P. Westbroek, T. Nyokong, *J. Photochem. Photobiol. A: Chemistry* **2012**, *240*, 50.
[98] H.-M. Wu, N. Chen, Z.-M. Wu, Z.-L. Chen, Y.-J. Yan, *J. Biomater. Appl.* **2013**, *27*, 773.
[99] G.-Y. Wan, Y. Liu, B.-W. Chen, Y.-Y. Liu, Y.-S. Wang, N. Zhang, *Cancer Biol. Med.* **2016**, *13*, 325.
[100] E. T. P. Ayala, F. A. D. de Sousa, J. D. Vollet-Filho, M. R. Garcia, L. De Boni, V. S. Bagnato, S. Pratavieira, *Ultrasound in Medicine & Biology* **2021**, *47*, 1032.
[101] Y. Su, S. M. Andrabi, S. S. Shahriar, S. L. Wong, G. Wang, J. Xie, *J. Controlled Release* **2023**, *356*, 131.
[102] Y. Feng, C. C. Tonon, S. Ashraf, T. Hasan, *Adv. Drug Delivery Rev.* **2021**, *177*, 113941.
[103] G. Jiang, G. Li, *Biotechnol. Prog.* **2012**, *28*, 215.
[104] S. L. Stanley, F. Scholle, J. Zhu, Y. Lu, X. Zhang, X. Situ, R. A. Ghiladi, *Nanomaterials* **2016**, *6*, 77.
[105] F. Ma, C.-W. Yuan, X.-X. Ren, C.-J. You, J.-H. Cao, D.-Y. Wu, *J. Photochem. Photobiol. A: Chemistry* **2018**, *355*, 267.
[106] H. Zhang, Z. Xu, Y. Mao, Y. Zhang, Y. Li, J. Lao, L. Wang, *Polymers* **2021**, *13*, 3942.
[107] S. Saghebasl, H. Amini, A. Nobakht, S. Haiaty, H. S. Bagheri, P. Hasanpour, M. Milani, S. Saghati, O. Naturi, M. Farhadi, R. Rahbarghazi, *J. Nanobiotechnol.* **2023**, *21*, 313.
[108] W. Zhou, Z. Jiang, X. Lin, Y. Chen, Q. Wu, J. Chen, F. Zhang, G. Xie, Y. Zhang, J. Lin, N. Guo, *ACS omega* **2024**, *9*, 29274.
[109] T. Wang, X.-F. Zhang, X. Lu, *J. Mol. Struct.* **2015**, *1084*, 319.
[110] S. Mapukata, J. Britton, O. L. Osifeko, T. Nyokong, *Photodiagn. Photodyn. Ther.* **2021**, *33*, 102100.
[111] A. Goethals, T. Mugadza, Y. Arslanoglu, R. Zugle, E. Antunes, S. W. Van Hulle, T. Nyokong, K. De Clerck, *J. Appl. Polym. Sci.* **2014**, *131*, 13.
[112] A. Severyukhina, N. Petrova, K. Smuda, G. Terentyuk, B. Klebtsov, R. Georgieva, H. Bäumler, D. Gorin, *Colloids Surf., B* **2016**, *144*, 57.
[113] A. Severyukhina, N. Petrova, A. Yashchenok, D. Bratashov, K. Smuda, I. Mamonova, N. Yurasov, D. Puchinyan, R. Georgieva, H. Bäumler, A. Lapanje, D. A. Gorin, *Mater. Sci. Eng: C* **2017**, *70*, 311.
[114] A. Galstyan, K. Strokov, *Photochem. Photobiol. Sci.* **2022**, *21*, 1387.
[115] T. Czapka, A. Winkler, I. Maliszewska, R. Kacprzyk, *Energies* **2021**, *14*, 2598.
[116] F.-C. Guo, C.-Y. Chen, *ACS Appl. Polym. Mater* **2022**, *4*, 4576.
[117] W.-Y. Chang, C.-Y. Chen, *ACS omega* **2023**, *8*, 36906.
[118] J. Sun, Y. Fan, P. Zhang, X. Zhang, Q. Zhou, J. Zhao, L. Ren, *J. Colloid Interface Sci.* **2020**, *559*, 197.
[119] J. Sun, P. Zhang, Y. Fan, J. Zhao, S. Niu, L. Song, L. Ma, L. Ren, W. Ming, *Mater. Sci. Eng: C* **2019**, *103*, 109797.
[120] C.-L. Liu, J. Yang, X.-H. Bai, Z.-K. Cao, C. Yang, S. Ramakrishna, D.-P. Yang, J. Zhang, Y.-Z. Long, *Nanoscale Res. Lett.* **2021**, *16*, 1.
[121] J. Zhang, C.-L. Liu, J.-J. Liu, X.-H. Bai, Z.-K. Cao, J. Yang, M. Yu, S. Ramakrishna, Y.-Z. Long, *Nanoscale* **2021**, *13*, 6105.
[122] X. Dong, D. G. Mitchell, M. Y. G. Cervantes, B. Chitara, L. Yang, F. Yan, *Environmental Science: Advances* **2022**, *1*, 736.
[123] S. Qian, L. Song, L. Sun, X. Zhang, Z. Xin, J. Yin, S. Luan, *J. Photochem. Photobiol. A: Chemistry* **2020**, *400*, 112626.
[124] H. Li, B. Sanchez-Vazquez, R. P. Trindade, Q. Zou, Y. Mai, L. Dou, L.-M. Zhu, G. R. Williams, *Colloids Surf. B: Biointerfaces* **2019**, *183*, 110411.
[125] T. L. Braga, A. R. de Souza Rossin, J. A. Fernandes, P. d. S. B. de Mendonça, L. V. de Castro-Hoshino, M. L. Baesso, C. F. de Freitas, E. Radovanovic, W. Caetano, *Applied Materials Today* **2024**, *36*, 102073.
[126] B. Gutberlet, E. Preis, V. Roschenko, U. Bakowsky, *Pharmaceutics* **2023**, *15*, 327.
[127] E. Preis, T. Anders, J. Širc, R. Hobzova, A.-I. Cocarta, U. Bakowsky, J. Jedelská, *Mater. Sci. Eng: C* **2020**, *115*, 111068.
[128] H. Qiu, S. Zhu, L. Pang, J. Ma, Y. Liu, L. Du, Y. Wu, Y. Jin, *Int. J. Pharm.* **2020**, *588*, 119797.
[129] L. Zhang, J. Yang, X. Zhu, X. Jia, Y. Liu, L. Cai, Y. Wu, H. Ruan, J. Chen, *Environ. Technol.* **2023**, *30*, 103098.
[130] G. Kabay, A. E. Meydan, T. Eom, B. S. Shim, M. Mutlu, G. Kaleli-Can, *Int. J. Pharm.* **2023**, *630*, 122442.
[131] E. Bayrak, P. Yiğit, E. Bakay, B. Sirek, N. Topaloğlu, E. Baysoy, G. Kaleli-Can, *Macromol. Mater. Eng.* **2024**, *309*, 2300382.
[132] S. Jiang, B. C. Ma, W. Huang, A. Kaltbeitzel, G. Kizisavas, D. Crespy, K. A. Zhang, K. Landfester, *Nanoscale Horiz.* **2018**, *3*, 439.
[133] J. Xiao, L. Cheng, T. Fang, Y. Zhang, J. Zhou, R. Cheng, W. Tang, X. Zhong, Y. Lu, L. Deng, Y. Cheng, Y. Zhu, Z. Liu, W. Cui, *Small* **2019**, *15*, 1904979.
[134] J. Xiao, Y. Zhang, T. Fang, T. Yuan, Q. Tian, J. Liu, Y. Cheng, Y. Zhu, L. Cheng, W. Cui, *Nano Res.* **2021**, *14*, 2145.
[135] X. Nie, S. Wu, A. Mensah, K. Lu, Q. Wei, *Mater. Sci. Eng: C* **2020**, *108*, 110377.
[136] K. Ghosal, M. Kováčová, P. Humpolíček, J. Vajďák, M. Bodík, Z. Špitalský, *Photodiagn. Photodyn. Ther.* **2021**, *35*, 102455.
[137] A. R. d. S. Rossin, J. Caetano, H. G. Zanella, R. A. Bariccatti, L. Gaffo, E. C. Muniz, W. Caetano, S. F. Stolf, D. C. Dragunski, *J. Therm. Anal. Calorim.* **2021**, 1.
[138] X. Liu, C. Guo, K. Zhuang, W. Chen, M. Zhang, Y. Dai, L. Tan, Y. Ran, *PLoS Pathog.* **2022**, *18*, e1010534.
[139] M. Pourhajibagher, M. Azimi, V. Haddadi-Asl, H. Ahmadi, M. Gholamzad, S. Ghorbanpour, A. Bahador, *Photodiagn. Photodyn. Ther.* **2021**, *34*, 102286.
[140] W.-C. Lin, I.-T. Yeh, E. Niyama, W.-R. Huang, M. Ebara, C.-S. Wu, *Polymers* **2018**, *10*, 231.
[141] H. P. Lee, A. K. Gaharwar, *Adv. Sci.* **2020**, *7*, 2000863.
[142] J. Sun, L. Song, Y. Fan, L. Tian, S. Luan, S. Niu, L. Ren, W. Ming, J. Zhao, *ACS Appl. Mater. Interfaces* **2019**, *11*, 26581.
[143] H. Lv, X. Xia, S. Sun, Z. Niu, J. Liu, X. Li, *Frontiers in Microbiology* **2024**, *15*, 1375956.
[144] S. Zhang, J. Ye, X. Liu, Y. Wang, C. Li, J. Fang, B. Chang, Y. Qi, Y. Li, G. Ning, *J. Colloid Interface Sci.* **2021**, *599*, 390.
[145] J. Yang, L. Xu, Y. Ding, C. Liu, B. Wang, Y. Yu, C. Hui, S. Ramakrishna, J. Zhang, Y. Long, *Adv. Fiber Mater.* **2023**, *5*, 209.
[146] H. Zhao, Y. Yang, J. An, H. Xin, Y. Xiao, Z. Jia, Y. Wu, L. Sheng, M. Wen, *ACS Appl. Nano Mater.* **2024**, *7*, 17707.
[147] M. Zhao, C. Liu, Z. Shan, C. Ji, X. Lu, G. Lv, *Frontiers in Chemistry* **2022**, *10*, 890545.
[148] S. Chen, B. Liu, M. A. Carlson, A. F. Gombart, D. A. Reilly, J. Xie, *Nanomedicine* **2017**, *12*, 1335.
[149] I. Behere, G. Ingavle, *J. Biomed. Mater. Res., Part A* **2022**, *110*, 443.
[150] X. Zhang, Y. Meng, B. Gong, T. Wang, Y. Lu, L. Zhang, J. Xue, *J. Mater. Chem. B* **2022**, *10*, 7281.
[151] J. Park, Y. Wu, J. S. Kim, J. Byun, J. Lee, Y.-K. Oh, *Adv. Drug Delivery Rev.* **2024**, 115362.
[152] Y. Guan, Y. Zhou, J. Sheng, Z. Ying Jiang, H. Jumahan, Y. Hu, *J. Chem. Technol. Biotechnol.* **2016**, *91*, 1128.
[153] B. Sanchez-Vazquez, A. J. Amaral, D.-G. Yu, G. Pasparakis, G. R. Williams, *Aaps Pharmscitech* **2017**, *18*, 1460.
[154] K. Dziemidowicz, S. Brocchini, G. R. Williams, *Int. J. Pharm.* **2021**, *597*, 120231.
[155] D. F. Suárez, A. D. Pinzón-García, R. D. Sinisterra, A. Dussan, F. Mesa, S. Ramírez-Clavijo, *Nanomaterials* **2022**, *12*, 3348.
[156] Y.-c. Liu, G.-j. Liu, W. Zhou, G.-l. Feng, Q.-y. Ma, Y. Zhang, G.-w. Xing, *Angew. Chem.* **2023**, *135*, e202309786.
[157] L. Flowers, E. A. Grice, *Cell Host Microbe* **2020**, *28*, 190.
[158] M. S. Linz, A. Mattappallil, D. Finkel, D. Parker, *Antibiotics* **2023**, *12*, 557.

[159] A. Atia, A. Ashour, N. Shaban, F. Omar, *Iberoam. J. Med.* **2021**, *3*, 3.
[160] P. Del Giudice, *Acta Derm.-Venereol.* **2020**, *100*, 9.
[161] V. Klepac-Ceraj, N. Patel, X. Song, C. Holewa, C. Patel, R. Kent, M. M. Amiji, N. S. Soukos, *Lasers in surgery and medicine* **2011**, *43*, 600.
[162] A. Taldaev, R. Terekhov, I. Nikitin, E. Melnik, V. Kuzina, M. Klochko, I. Reshetov, A. Shiryaev, V. Loschenov, G. Ramenskaya, *Frontiers in Pharmacology* **2023**, *14*, 1264961.
[163] L. Shang, X. Zhou, J. Zhang, Y. Shi, L. Zhong, *Molecules* **2021**, *26*, 6532.
[164] M. Bakht, S. A. Alizadeh, S. Rahimi, R. Kazemzadeh Anari, M. Rostamani, A. Javadi, A. Peymani, S. M. A. Marashi, F. Nikkhahi, *BMC Microbiol.* **2022**, *22*, 124.
[165] C. Tong, H. Hu, G. Chen, Z. Li, A. Li, J. Zhang, *Environ. Res.* **2021**, *199*, 111296.
[166] B. Nagoba, M. Davane, R. Gandhi, B. Wadher, N. Suryawanshi, S. Selkar, *Wound Medicine* **2017**, *19*, 5.
[167] J. Lee, S. Moon, J. Lahann, K. J. Lee, *Macromol. Mater. Eng.* **2023**, *308*, 2300057.
[168] A. Kühbacher, A. Burger-Kentischer, S. Rupp, *Microorganisms* **2017**, *5*, 32.
[169] D. O. Thomas-Rüddel, P. Schlattmann, M. Pletz, O. Kurzai, F. Bloos, *Chest* **2022**, *161*, 345.
[170] S. R. Lockhart, A. Chowdhary, J. A. Gold, *Nat. Rev. Microbiol.* **2023**, *21*, 818.
[171] X. Wu, Y. Hu, *Infection and drug resistance* **2022**, 3251.
[172] A. Sanyaolu, C. Okorie, A. Marinkovic, A. F. Abbasi, S. Prakash, J. Mangat, Z. Hosein, N. Haider, J. Chan, *Infect. Chemother.* **2022**, *54*, 236.
[173] A. Chowdhary, A. Prakash, C. Sharma, M. Kordalewska, A. Kumar, S. Sarma, B. Tarai, A. Singh, G. Upadhyaya, S. Upadhyay, P. Yadav, P. K. Singh, V. Khillan, N. Sachdeva, D. S. Perlin, J. F. Meis, *J. Antimicrob. Chemother.* **2018**, *73*, 891.
[174] Y. Seo, K. Park, Y. Hong, E. S. Lee, S.-S. Kim, Y.-T. Jung, H. Park, C. Kwon, Y.-S. Cho, Y.-D. Huh, *Journal of Analytical Science and Technology* **2020**, *11*, 1.
[175] N. Kojima, L. Peterson, R. Hawkins, M. Allen, B. Flannery, T. M. Uyeki, *JAMA* **2023**, *330*, 1793.
[176] A. Wiehe, J. M. O'Brien, M. O. Senge, *Photochem. Photobiol. Sci.* **2019**, *18*, 2565.
[177] L. Sobotta, P. Skupin-Mrugalska, J. Mielcarek, T. Goslinski, J. Balzarini, *Mini reviews in medicinal chemistry* **2015**, *15*, 503.
[178] M. S. Maginnis, *J. Mol. Biol.* **2018**, *430*, 2590.
[179] L. Marciel, L. Teles, B. Moreira, M. Pacheco, L. M. Lourenco, M. G. Neves, J. P. Tome, M. A. Faustino, A. Almeida, *Future Med. Chem.* **2017**, *9*, 365.
[180] Y. Yang, S. Ma, A. Li, G. Xia, M. Li, C. Ding, X. Sun, L. Yan, M. Yang, T. Zhao, *Frontiers in Bioengineering and Biotechnology* **2024**, *12*, 1428988.
[181] R. Chen, C. Zhao, Z. Chen, X. Shi, H. Zhu, Q. Bu, L. Wang, C. Wang, H. He, *Biomaterials* **2022**, *281*, 121330.
[182] X. Wei, M. Li, Z. Zheng, J. Ma, Y. Gao, L. Chen, Y. Peng, S. Yu, L. Yang, *Burns & trauma* **2022**, *10*, tkab045.
[183] A. D. J. Bombin, N. J. Dunne, H. O. McCarthy, *Mater. Sci. Eng: C* **2020**, *114*, 110994.
[184] Z. Jiang, Z. Zheng, S. Yu, Y. Gao, J. Ma, L. Huang, L. Yang, *Pharmaceutics* **2023**, *15*, 1829.
[185] H. Samadian, S. Zamiri, A. Ehterami, S. Farzamfar, A. Vaez, H. Khastar, M. Alam, A. Ai, H. Derakhshankhah, Z. Allahyari, A. Goodarzi, M. Salehi, *Sci. Rep.* **2020**, *10*, 8312.
[186] S. a. Guo, L. A. DiPietro, *J. Dent. Res.* **2010**, *89*, 219.
[187] R. M. Sabino, K. C. Popat, *Bio-protocol* **2020**, *10*, e3505.
[188] J.-C. Park, T. Ito, K.-O. Kim, K.-W. Kim, B.-S. Kim, M.-S. Khil, H.-Y. Kim, I.-S. Kim, *Polym. J.* **2010**, *42*, 273.
[189] X. Hu, L. Yang, Y. Zhang, B. Shou, H.-T. Ren, J.-H. Lin, C.-W. Lou, T.-T. Li, *Int. J. Biol. Macromol.* **2023**, *253*, 126737.
[190] L. El-Khordagui, N. El-Sayed, S. Galal, H. El-Gowelli, H. Omar, M. Mohamed, *Int. J. Pharm.* **2017**, *520*, 139.
[191] J. Ghorbani, D. Rahban, S. Aghamiri, A. Teymouri, A. Bahador, *Laser therapy* **2018**, *27*, 293.
[192] C. C. Tonon, S. Ashraf, J. Q. Alburquerque, A. N. de Souza Rastelli, T. Hasan, A. M. Lyons, A. Greer, *J. Photochem. Photobiol.* **2021**, *97*, 1266.
[193] D. Aebisher, I. Serafin, K. Batég-Szczech, K. Dynarowicz, E. Chodurek, A. Kawczyk-Krupka, D. Bartusik-Aebisher, *Pharmaceuticals* **2024**, *17*, 932.
[194] S. K. Sharma, P. Mroz, T. Dai, Y.-Y. Huang, T. G. S. Denis, M. R. Hamblin, *Isr. J. Chem.* **2012**, *52*, 691.
[195] R. Zhou, X. Zeng, H. Zhao, Q. Chen, P. Wu, *Coord. Chem. Rev.* **2022**, *452*, 214306.
[196] X. Shi, C. Y. Zhang, J. Gao, Z. Wang, *Wiley Interdiscip. Rev.: Nanomed. Nanobiotechnol.* **2019**, *11*, e1560.
[197] H. Xin, Y. Liu, Y. Xiao, M. Wen, L. Sheng, Z. Jia, *Adv. Funct. Mater.* **2024**, 2402607.
[198] Y. Li, J. Zhu, H. Cheng, G. Li, H. Cho, M. Jiang, Q. Gao, X. Zhang, *Adv. Funct. Mater.* **2021**, *6*, 2100410.
[199] R. Baskaran, J. Lee, S.-G. Yang, *Biomater. Res.* **2018**, *22*, 25.

Aslı Eldem graduated from the Department of Molecular Biology and Genetics at Uşak University and received her Ph.D. in Medical Biology from İzmir Katip Çelebi University in 2023. She is currently a postdoctoral researcher in the Department of Analytical Chemistry at the Faculty of Pharmacy, İzmir Katip Çelebi University. Her research interests include molecular biology, cancer biology, and immunology.

Yamac Tekintas obtained his M.Sc. and Ph.D. in Pharmaceutical Microbiology from Ege University in 2018. He is currently an Assistant Professor at the Faculty of Pharmacy, Izmir Katip Çelebi University. His research focuses on non-traditional antibacterial therapy.

Muhammed Ucuncu earned his Ph.D. in Organic Chemistry from the Izmir Institute of Technology in 2016, focusing on the development of fluorescent probes for heavy metal detection. He conducted his postdoctoral research in Mark Bradley's group at the School of Chemistry, University of Edinburgh, working on fluorescent smart probes for pathogen detection. Currently, he is an Associate Professor in the Faculty of Pharmacy at İzmir Katip Çelebi University. Dr. Ucuncu's expertise spans organic chemistry, spectroscopy, and photodynamic therapy, with a research focus on designing advanced "smart probes" for both diagnostic and therapeutic applications.

Nesrin Horzum received her chemistry degree from Pamukkale University in 2004 and completed her M.Sc. and Ph.D. at the Izmir Institute of Technology in 2013, focusing on electrospun nanofibers for filtration. During her Ph.D., she worked with Prof. K. Landfester at the Max Planck Institute for Polymer Research on colloid electrospinning. In 2014, she joined Prof. Bo Liedberg's group at Nanyang Technological University, researching paper-based sensors. Currently, she is a professor at Izmir Kâtip Çelebi University. Her research interests include the development of nanofibrous biomaterials and green nanocomposites for health and environmental applications.

